

*Ferroplasma acidarmanus*, methanethiol has been demonstrated, while its draft genome apparently lacks a gene encoding MGL or similar enzymes (The UCSC Archaeal Genome Browser at <http://archaea.ucsc.edu/>). Thus, it is feasible that in *F. acidarmanus*, methionine is degraded in two step reactions consisting an amino transfer, which yields 4-methylthio-2-oxobutyric acid, and chemical decompose into 2-oxobutyrate, as proposed for methionine catabolic pathway in yeast *Geotrichum candidum* (44).

## DRUG DEVELOPMENT EXPLOITING MGL

### Mechanisms of Trifluoromethionine (TFM) Targeting MGL in Pathogens

The emergence of drug resistance and adverse effects of available chemotherapeutics always necessitate discovery and development of new drugs targeting unexplored enzymes and pathways. The unique catalytic reaction of MGL and its limited distribution in pathogens, but not in human, makes the enzyme a promising target to design novel chemotherapeutic agents against amebiasis, trichomoniasis, and gum diseases (51, 52). Trifluoromethionine (*S*-trifluoromethyl-L-homocysteine, TFM), a fluorinated methionine in which three hydrogens of the methyl group are replaced by fluorines, was designed in the wake of successful use of metabolite analog such as 6-mercaptopurine (53).

Microbicidal mechanisms of TFM have been proposed. One of the products of TFM degraded by MGL, trifluoromethanethiol (trifluoromethylmercaptan), is converted non-enzymatically to carbonothionic difluoride, subsequently crosslinks the primary amino group of proteins, and causes toxicity (35, 54). We reported that TFM was preferentially degraded by one of the two *E. histolytica* isozymes, *EhMGL2*, and less efficiently by *EhMGL1* (35). Site-directed mutagenesis of *EhMGL1* and *EhMGL2* indicated that mechanisms of degradation differed between TFM and physiological substrates. Interestingly, the MGL mutants where the arginine residue that plays a critical role in the fixation of PLP was replaced by alanine, still retained activities against TFM, while they lost activities toward physiological substrates. These results imply that the degradation of TFM probably proceeds without interaction with other amino acid residues, possibly due to the electronegativity of the trifluoromethyl group of TFM (35).

### Antimicrobial Spectrum of TFM

TFM is highly toxic to various anaerobic microorganisms. The minimal inhibitory concentrations against *Mycobacterium smegmatis*, *Mycobacterium phlei*, and *Candida lipolytica* were estimated to be 24.6–49.3  $\mu\text{M}$  (55). The growth of periodontal bacteria *P. gingivalis* and *F. nucleatum* was retarded by 0.1 mM TFM and completely inhibited by 1 mM (56). *T. vaginalis* was killed at 24.6  $\mu\text{M}$  within 24 h *in vitro* (57). The  $\text{IC}_{50}$  value of TFM against the *E. histolytica* *in vitro* culture was

estimated to be 7.3  $\mu\text{M}$ , comparable to metronidazole, the commonly used drug (58).

The efficacy of TFM has also been tested *in vivo*. The single intravenous administration of 40 mg/kg of TFM to mice infected by the subcutaneous inoculation of *T. vaginalis* 2 h before the TFM treatment caused the lesion to be almost cured (five of six TFM-treated mice produced no lesion) (57). Survival rate of mice that received subcutaneous inoculation of *P. gingivalis* 3 days prior increased by 3.2-fold when coinjected with 4  $\mu\text{mol}$  of TFM (56). A single subcutaneous and oral administration of TFM (1.02 and 2.54 mg/kg each) after 24 h of intrahepatic inoculation of *E. histolytica* trophozoites also cured amoebic liver abscesses in hamsters (58).

### Selectivity of TFM

TFM is a prodrug which shows toxicity only after degradation by MGL. In fact, TFM showed no growth retardation or killing to MGL-deficient *P. gingivalis* (17). The growth inhibition of *T. vaginalis* by TFM was abolished by propargylglycine, a suicide substrate of MGL (57). Growth of *Giardia lamblia*, the parasite of duodenum and small intestine that causes watery diarrhea, and shares anaerobic energy metabolism with *E. histolytica* and *T. vaginalis*, but lacks MGL, was affected by only very high concentration of TFM (493  $\mu\text{M}$ ) (57). The growth of *E. coli* expressing *T. vaginalis* MGL was inhibited by TFM in a dose-dependent manner (57), while wild type *E. coli* was not affected by TFM (56). Although *E. coli* has cystathionine gamma-lyase and cystathionine gamma-synthase, both of which are structurally similar to MGL (32), TFM does not affect growth of *E. coli*.

Although TFM is structurally very similar to methionine, both utilization of TFM via the methionine cycle, initiated by methionine adenosyltransferase, and incorporation into proteins are extremely poor (59, 60). Furthermore, TFM did not affect the mammalian cystathionine gamma-lyase (54). In addition, TFM has little cytotoxic effect on mammalian cells. TFM at 493  $\mu\text{M}$  did not inhibit the growth of mouse myeloma cells (57) and CHO cells [the  $\text{IC}_{50}$  against CHO cells was 709  $\mu\text{M}$  (58)]. These data support that cytotoxic effects of TFM is specific to MGL and reinforce the selectivity of TFM against pathogens harboring MGL.

### Derivatization of TFM to Improve Efficacy

To improve the cytotoxicity of TFM, we synthesized various amide derivatives of TFM. Several TFM amide derivatives showed higher cytotoxic effects against *E. histolytica* *in vitro* compared to TFM and metronidazole (58). Kinetic studies with recombinant enzymes showed that the TFM amide derivatives were degraded by MGL, less efficiently compared to TFM. TFM amide derivatives appeared to be first hydrolyzed by cysteine proteases and metalloproteases in amoebic cell lysate, and subsequently degraded by the  $\alpha$ ,  $\gamma$ -elimination by MGL (58).

These results should help us to further improve the efficiency of TFM.

### Novel MGL Inhibitor

Recently, it has been shown that myrsinoic acid B, a terpenobenzoic acid, extracted from *the leaves of Myrsine Seguinii* Lév, has an inhibitory effect on MGL activity (61). It is thus the first natural MGL inhibitor reported. Myrsinoic acid B was also reported to possess anti-inflammatory activity against edema of mouse ear induced by skin tumor promoter (62). Myrsinoic acid B inhibited the production of 2-oxobutyrate in the crude extract of periodontal bacteria, *F. nucleatum*, *P. gingivalis*, and *T. denticola*. The IC<sub>50</sub> values of myrsinoic acid B against these bacteria were estimated to be 0.389  $\mu$ M, 82.4  $\mu$ M, or 30.3  $\mu$ M, respectively. Thus, these MGL inhibitors would be potentially useful for the prevention of oral malodor and periodontal diseases. For practical applications, it is important to show the specificity of myrsinoic acid B, and to exclude a possibility that it affects mammalian  $\gamma$ -family members of PLP-enzymes.

The physiological role of myrsinoic acid B in plants has not been demonstrated, similar to many other secondary metabolites. Assumed that myrsinoic acid B inhibits the endogenous MGL in *Myrsine Seguinii* Lév, it may control isoleucine synthesis by repressing methionine degradation. The other possibility is that myrsinoic acid B negatively regulates the release of methanethiol to allow inhabitation or parasitization by insects. It may be worth comparing the concentration of myrsinoic acid B and the MGL activity between intact and wounded leaves.

## UTILIZATION OF MGL FOR THE TREATMENT OF CANCERS

### Rationale of MGL for Cancer Treatment

Many cancer cells have an absolute requirement for plasma methionine, whereas normal cells are relatively resistant to the restriction of exogenous methionine (63). Methionine depletion has a broad spectrum of antitumor activities (64). Under methionine depletion, cancer cells were arrested in the late S-G2 phase due to the pleiotropic effects and underwent apoptosis. Thus, therapeutic exploitation of *P. putida* MGL to deplete plasma methionine has been extensively investigated (64). Growth of various tumors such as Lewis lung carcinoma (65), human colon cancer lines (66), glioblastoma (67), and neuroblastoma (68) was arrested by MGL. MGL in combination with anticancer drugs such as cisplatin, 5-fluorouracil, nitrosourea, and vincristine displayed synergistic antitumor effects on rodent and human tumors in mouse models (65–68). It was also reported that MGL introduced by adenovirus vector inhibited the growth of tumors *in vitro*. MGL, when combined with selenomethionine, a suicide prodrug substrate of MGL, inhibited tumor growth in rodents and prolonged their survivals (69). Methaneselenol produced by decomposition of selenomethionine, was oxidized to methylseleninic acid, which in turn oxidized

protein sulfhydryls and generated reactive oxygen species, and was then reduced back to selenol by glutathione (70). In addition to the synergistic effects noted above, the advantage of anticancer therapy using MGL is its wide range of target tumors, including those resistant to the conventional chemotherapeutics and radiation. Taken together, MGL treatment will provide a novel paradigm for cancer therapy.

### Modifications of MGL to Reduce its Side Effects

It was reported that administration of MGL caused anaphylactic shock in macaque monkeys (71). To overcome this problem, polyethylene glycol-conjugated MGL (PEG-MGL) was constructed. PEG-MGL reduced immunogenicity; the IgG titers decreased by 10 to 10,000-fold, depending on the binding rate of PEG and MGL, compared to naked MGL. The half life and depletion time of MGL in the mouse plasma was improved by PEG conjugation. The enzymatic activity of PEG-MGL was detected for 72 h, while that of unconjugated MGL was undetectable after 24 h, and the half life of PEG-MGL increased by  $\sim$ 20 times (38 h), compared to unconjugated MGL (2 h) (72). Simultaneous coadministration of pyridoxal 5'-phosphate and oleic acid, or dithiothreitol treatment also strengthened effectiveness of PEG-MGL in the rodent model (72, 73).

## OTHER APPLICATIONS OF MGL

Elevated blood and serum homocysteine is known as a notorious risk factor for cardio-vascular diseases, dementia, and Alzheimer's disease (74). It was reported that the administration of the combination of vitamins (folic acid, vitamins B<sub>6</sub>, and B<sub>12</sub>) decreased homocysteine concentrations, but did not significantly reduce the risk of death from cardio-vascular diseases (75–77). Thus, therapeutic interventions by directly lowering homocysteine by the administration of MGL may be worth attempting.

The unique enzymological properties of MGL was applied to clinical examination of homocysteine, cysteine, and PLP (78–80). These examination methods utilizing MGL with sufficient sensitivities are suitable for mass screening and, thus, can be an economical alternate of the expensive HPLC-dependent method.

## PERSPECTIVES

Although MGL has been explored to be an ideal drug target against microbial infections and also for the treatment of cancers, its reaction mechanism and physiological functions remain to be fully elucidated. Recently structural analyzes of wild type and mutant MGLs have been reported (26, 35, 37), which disclose the substrate recognition and reaction mechanisms. In addition, the tertiary structures of MGLs were resolved (24–26, 28–30) PDB ID: 1E5F and 1PFF), including the complex with inhibitors (PDB ID, 1E5E; Harada, et al., unpublished). To further elucidate the reaction mechanisms, the tertiary structures of various stages of the MGL-substrate/prodrug/inhibitor complex need to be resolved. These data should lead to a further fine

adjustment of anti-infective agents targeting MGL and anti-cancer drugs exploiting MGL.

The acquisition and conservation of MGL in a limited lineage of bacteria and archaea remain one of the major unsolved issues. Manukhov et al. reported that the *C. freundii* has a MGL gene while its vestigial gene was found in the other bacteria in Enterobacteriaceae family, such as *Salmonella enterica* serovar Typhimurium, *Shigella flexneri*, *E. coli*, and *C. rodentium* (81). These bacteria appear to have acquired MGL by lateral gene transfer from a common ancestor, and the latter have lost the function of MGL. To compensate the secondary loss of MGL, these bacteria might utilize an alternative pathway, as shown in yeast *G. candidum*. In this pathway, methionine degradation is initiated by transamidation, which forms 4-methylthio-2-oxobutyrate, followed by a cleavage to yield 2-oxobutyrate and methanethiol by chemical process (44). The comparative metabolomics and fluxomics between the bacteria possessing or lacking MGL should help our understanding its biological importance of MGLs.

As far as the genome is available, only the unicellular parasitic protozoa possess two MGL isozymes with distinct substrate specificities. This unique redundancy might be related to the parasitic life styles, for example, the acquisition of nutrients from the human host and the complex life cycle. Reverse genetic approaches (82, 83) or specific inhibitors, in combination with "omics" approaches including metabolomics/transcriptomics should delineate individual roles of the isotypes.

#### ACKNOWLEDGEMENTS

The authors thank Dr. Shigeharu Harada and Mr. Tsuyoshi Karaki, Department of Applied Biology, Kyoto Institute of Technology, for kindly permitting them to use the images of crystal structures of *E. histolytica* MGL. This work was supported by a Grant-in-Aid for Scientific Research from the Ministry of Education, Culture, Sports, Science and Technology of Japan to D.S. (20590429) and T.N. (18GS0314, 18050006, 18073001), a grant for research on emerging and re-emerging infectious diseases from the Ministry of Health, Labor and Welfare of Japan (H20-Shinkosaiko-016), and a grant for research to promote the development of anti-AIDS pharmaceuticals from the Japan Health Sciences Foundation to T.N.

#### REFERENCES

- Nozaki, T., Ali, V., and Tokoro, M. (2005) Sulfur-containing amino acid metabolism in parasitic protozoa. *Adv. Parasitol.* **60**, 1–99.
- Stipanuk, M. H. (2004) Sulfur amino acid metabolism: pathways for production and removal of homocysteine and cysteine. *Annu. Rev. Nutr.* **24**, 539–577.
- De Bree, A., Verschuren, W. M., Kromhout, D., Kluijtmans, L. A., and Blom, H. J. (2002) Homocysteine determinants and the evidence to what extent homocysteine determines the risk of coronary heart disease. *Pharmacol. Rev.* **54**, 599–618.
- Wald, D. S., Law, M., and Morris, J. K. (2002) Homocysteine and cardiovascular disease: evidence on causality from a meta-analysis. *BMJ* **325**, 1202–1206.
- Morris, M. S. (2003) Homocysteine and Alzheimer's disease. *Lancet. Neurol.* **2**, 425–428.
- Joseph, C. A. and Maroney, M. J. (2007) Cysteine dioxygenase: structure and mechanism. *Chem. Commun. (Camb.)* 3338–3349.
- Uren, J. R. (1987) Cystathionine beta-lyase from *Escherichia coli*. *Methods. Enzymol.* **143**, 483–486.
- Ravanel, S., Job, D., and Douce, R. (1996) Purification and properties of cystathionine beta-lyase from *Arabidopsis thaliana* overexpressed in *Escherichia coli*. *Biochem. J.* **320**, 383–392.
- Onitake, J. (1938) On the formation of methyl mercaptan from L-cystine and L-methionine by bacteria. *J. Osaka Med. Assoc.* **37**, 263–270.
- Kreis, W. and Hession, C. (1973) Isolation and purification of L-methionine-alpha-deamino-gamma-mercaptomethane-lyase (L-methioninase) from *Clostridium sporogenes*. *Cancer. Res.* **33**, 1862–1865.
- Tanaka, H., Esaki, N., and Soda, K. (1977) Properties of L-methionine gamma-lyase from *Pseudomonas ovalis*. *Biochemistry* **16**, 100–106.
- Nakayama, T., Esaki, N., Sugie, K., Beresov, T. T., Tanaka, H., and Soda, K. (1984) Purification of bacterial L-methionine gamma-lyase. *Anal. Biochem.* **138**, 421–424.
- Nakayama, T., Esaki, N., Lee, W.-J., Tanaka, I., Tanaka, H., and Soda, K. (1984) Purification and properties of L-methionine gamma-lyase from *Aeromonas* sp. *Agric. Biol. Chem.* **48**, 2367–2369.
- Faleev, N. G., Troitskaya, M. V., Paskonova, E. A., Saporovskaya, M. B., and Belikov, V. M. (1996) L-methionine-gamma-lyase in *Citrobacter intermedium* cells: stereochemical requirements with respect to the thiol structure. *Enzyme. Microb. Technol.* **19**, 590–593.
- Dias, B. and Weimer, B. (1998) Purification and characterization of L-methionine gamma-lyase from *Brevibacterium linens* BL2. *Appl. Environ. Microbiol.* **64**, 3327–3331.
- Manukhov, I. V., Mamaeva, D. V., Morozova, E. A., Rastorguev, S. M., Faleev, N. G., Demidkina, T. V., and Zavilgelsky, G. B. (2006) L-methionine gamma-lyase from *Citrobacter freundii*: cloning of the gene and kinetic parameters of the enzyme. *Biochemistry (Mosc.)* **71**, 361–369.
- Yoshimura, M., Nakano, Y., Yamashita, Y., Oho, T., Saito, T., and Koga, T. (2000) Formation of methyl mercaptan from L-methionine by *Porphyromonas gingivalis*. *Infect. Immun.* **68**, 6912–6916.
- Fukamachi, H., Nakano, Y., Okano, S., Shibata, Y., Abiko, Y., and Yamashita, Y. (2005) High production of methyl mercaptan by L-methionine-alpha-deamino-gamma-mercaptomethane lyase from *Treponema denticola*. *Biochem. Biophys. Res. Commun.* **331**, 127–131.
- Lockwood, B. C. and Coombs, G. H. (1991) Purification and characterization of methionine gamma-lyase from *Trichomonas vaginalis*. *Biochem. J.* **279**, 675–682.
- Tokoro, M., Asai, T., Kobayashi, S., Takeuchi, T., and Nozaki, T. (2003) Identification and characterization of two isoenzymes of methionine gamma-lyase from *Entamoeba histolytica*: a key enzyme of sulfur-amino acid degradation in an anaerobic parasitic protist that lacks forward and reverse trans-sulfuration pathways. *J. Biol. Chem.* **278**, 42717–42727.
- Rébeillé, F., Jabrin, S., Bligny, R., Loizeau, K., Gambonnet, B., Van Wilder, V., Douce, R., and Ravanel, S. (2006) Methionine catabolism in *Arabidopsis cells* is initiated by a gamma-cleavage process and leads to S-methylcysteine and isoleucine syntheses. *Proc. Natl. Acad. Sci. USA* **103**, 15687–15692.
- Baumler, D. J., Hung, K. F., Jeong, K. C., and Kaspar, C. W. (2007) Production of methanethiol and volatile sulfur compounds by the archaeon "Ferroplasma acidarmanus." *Extremophiles* **11**, 841–851.
- Bonnarme, P., Psoni, L., and Spinnler, H. E. (2000) Diversity of L-methionine catabolism pathways in cheese-ripening bacteria. *Appl. Environ. Microbiol.* **66**, 5514–5517.
- Motoshima, H., Inagaki, K., Kumasaka, T., Furuichi, M., Inoue, H., Tamura, T., Esaki, N., Soda, K., Tanaka, N., Yamamoto, M., and Tanaka, H. (2000) Crystal structure of the pyridoxal 5'-phosphate

- dependent L-methionine gamma-lyase from *Pseudomonas putida*. *J. Biochem. (Tokyo)* **128**, 349–354.
25. Sridhar, V., Xu, M., Han, Q., Sun, X., Tan, Y., Hoffman, R. M., and Prasad, G. S. (2000) Crystallization and preliminary crystallographic characterization of recombinant L-methionine-alpha-deamino-gamma-mercaptomethane lyase (methioninase). *Acta. Crystallogr. D. Biol. Crystallogr.* **56**, 1665–1667.
  26. Kudou, D., Misaki, S., Yamashita, M., Tamura, T., Takakura, T., Yoshioka, T., Yagi, S., Hoffman, R. M., Takimoto, A., Esaki, N., and Inagaki, K. (2007) Structure of the antitumor enzyme L-methionine gamma-lyase from *Pseudomonas putida* at 1.8 Å resolution. *J. Biochem. (Tokyo)* **141**, 535–544.
  27. Mamaeva, D. V., Morozova, E. A., Nikulin, A. D., Revtovich, S. V., Nikonov, S. V., Garber, M. B., and Demidkina, T. V. (2005) Structure of *Citrobacter freundii*-methionine gamma-lyase. *Acta. Crystallogr. Sect. F Struct. Biol. Cryst. Commun.* **61**, 546–549.
  28. Nikulin, A., Revtovich, S., Morozova, E., Nevskaya, N., Nikonov, S., Garber, M., and Demidkina, T. (2008) High-resolution structure of methionine gamma-lyase from *Citrobacter freundii*. *Acta. Crystallogr. D. Biol. Crystallogr.* **64**, 211–218.
  29. Sato, D., Yamagata, W., Kamei, K., Nozaki, T., and Harada, S. (2006) Expression, purification and crystallization of L-methionine gamma-lyase 2 from *Entamoeba histolytica*. *Acta. Crystallogr. Sect. F Struct. Biol. Cryst. Commun.* **62**, 1034–1036.
  30. Sato, D., Karaki, T., Shimizu, A., Kamei, K., Harada, S., and Nozaki, T. (2008) Crystallization and preliminary x-ray analysis of L-methionine gamma-lyase 1 from *Entamoeba histolytica*. *Acta. Crystallogr. Sect. F Struct. Biol. Cryst. Commun.* **64**, 697–699.
  31. Tanaka, H., Esaki, N., and Soda, K. (1985) A versatile bacterial enzyme: L-methionine  $\gamma$ -lyase. *Enzyme. Microb. Technol.* **7**, 530–537.
  32. Alexander, F. W., Sandmeier, E., Mehta, P. K., and Christen, P. (1994) Evolutionary relationships among pyridoxal-5'-phosphate-dependent enzymes. Regio-specific alpha, beta and gamma families. *Eur. J. Biochem.* **219**, 953–960.
  33. Inoue, H., Inagaki, K., Adachi, N., Tamura, T., Esaki, N., Soda, K., and Tanaka, H. (2000) Role of tyrosine 114 of L-methionine gamma-lyase from *Pseudomonas putida*. *Biosci. Biotechnol. Biochem.* **64**, 2336–2343.
  34. Toney, M. D. (2005) Reaction specificity in pyridoxal phosphate enzymes. *Arch. Biochem. Biophys.* **433**, 279–287.
  35. Sato, D., Yamagata, W., Harada, S., and Nozaki, T. (2008) Kinetic characterization of methionine gamma-lyases from the enteric protozoan parasite *Entamoeba histolytica* against physiological substrates and trifluoromethionine, a promising lead compound against amoebiasis. *FEBS. J.* **275**, 548–560.
  36. Inoue, H., Inagaki, K., Sugimoto, M., Esaki, N., Soda, K., and Tanaka, H. (1995) Structural analysis of the L-methionine gamma-lyase gene from *Pseudomonas putida*. *J. Biochem. (Tokyo)* **117**, 1120–1125.
  37. Kudou, D., Misaki, S., Yamashita, M., Tamura, T., Esaki, N., and Inagaki, K. (2008) The role of cysteine 116 in the active site of the antitumor enzyme L-methionine gamma-lyase from *Pseudomonas putida*. *Biosci. Biotechnol. Biochem.* **72**, 1722–1730.
  38. Goyer, A., Collakova, E., Shachar-Hill, Y., and Hanson, A. D. (2007) Functional characterization of a methionine  $\gamma$ -Lyase in *Arabidopsis* and its implication in an alternative to the reverse trans-sulfuration pathway. *Plant. Cell. Physiol.* **48**, 232–242.
  39. Mckie, A. E., Edlind, T., Walker, J., Mottram, J. C., and Coombs, G. H. (1998) The primitive protozoan *Trichomonas vaginalis* contains two methionine gamma-lyase genes that encode members of the gamma-family of pyridoxal 5'-phosphate-dependent enzymes. *J. Biol. Chem.* **273**, 5549–5556.
  40. Nakayama, T., Esaki, N., Tanaka, H., and Soda, K. (1988) Specific labeling of the essential cysteine residue of L-methionine gamma-lyase with a cofactor analog, N-(bromoacetyl)pyridoxamine phosphate. *Biochemistry* **27**, 1587–1591.
  41. Nakayama, T., Esaki, N., Tanaka, H., and Soda, K. (1988) Chemical modification of cysteine residues of L-methionine  $\gamma$ -lyase. *Agric. Biol. Chem.* **52**, 177–183.
  42. Ragsdale, S. W. (2003) Pyruvate ferredoxin oxidoreductase and its radical intermediate. *Chem. Rev.* **103**, 2333–2346.
  43. Müller, M., Coombs, G. H., Vickerman, K., Sleight, M. A. and, Warren, A., eds. (1998) *Enzymes and Compartmentation of Core Energy Metabolism of Anaerobic Protists—A Special Case in Eukaryotic Evolution?* In *Evolutionary relationships among protozoa*. (Coombs, G.H., Vickerman, K., Sleight, M.A., Warren, A., ed) pp. 109–131. Kluwer Academic Publishers, London.
  44. Arfi, K., Landaud, S., and Bonnarne, P. (2006) Evidence for distinct L-methionine catabolic pathways in the yeast *Geotrichum candidum* and the bacterium *Brevibacterium linens*. *Appl. Environ. Microbiol.* **72**, 2155–2162.
  45. Cholet, O., Hénaut, A., and Bonnarne, P. (2007) Transcriptional analysis of L-methionine catabolism in *Brevibacterium linens* ATCC9175. *Appl. Microbiol. Biotechnol.* **74**, 1320–1332.
  46. Rouseff, R. L., Onagbola, E. O., Smoot, J. M., and Stelinski, L. L. (2008) Sulfur volatiles in guava (*Psidium guajava* L.) leaves: possible defense mechanism. *J. Agric. Food. Chem.* **56**, 8905–8910.
  47. Inoue, H., Inagaki, K., Eriguchi, S. I., Tamura, T., Esaki, N., Soda, K., and Tanaka, H. (1997) Molecular characterization of the *mde* operon involved in L-methionine catabolism of *Pseudomonas putida*. *J. Bacteriol.* **179**, 3956–3962.
  48. Inoue, H., Nishito, A., Eriguchi, S. I., Tamura, T., Inagaki, K., and Tanaka, H. (2003) Purification and substrate characterization of  $\alpha$ -keto-butyrate decarboxylase from *Pseudomonas putida*. *J. Mol. Catal., B Enzym.* **23**, 265–271.
  49. Rosenthal, B., Mai, Z., Caplivski, D., Ghosh, S., De La Vega, H., Graf, T., and Samuelson, J. (1997) Evidence for the bacterial origin of genes encoding fermentation enzymes of the amitochondriate protozoan parasite *Entamoeba histolytica*. *J. Bacteriol.* **179**, 3736–3745.
  50. Mudd, S. H., Finkelstein, J. D., Refsum, H., Ueland, P. M., Malinow, M. R., Lentz, S. R., Jacobsen, D. W., Brattstrom, L., Wilcken, B., Wilcken, D. E., Blom, H. J., Stabler, S. P., Allen, R. H., Selhub, J., and Rosenberg, I. H. (2000) Homocysteine and its disulfide derivatives: a suggested consensus terminology. *Arterioscler. Thromb. Vasc. Biol.* **20**, 1704–1706.
  51. Ali, V. and Nozaki, T. (2007) Current therapeutics, their problems, and sulfur-containing-amino-acid metabolism as a novel target against infections by “amitochondriate” protozoan parasites. *Clin. Microbiol. Rev.* **20**, 164–187.
  52. Nakano, Y., Yoshimura, M., and Koga, T. (2002) Methyl mercaptan production by periodontal bacteria. *Int. Dent. J.* **52**, 217–220.
  53. Dannley, R. L. and Taborsky, R. G. (1957) Synthesis of DL-S-trifluoromethylhomocysteine (trifluoromethylmethionine). *J. Org. Chem.* **22**, 1275–1276.
  54. Alston, T. A. and Bright, H. J. (1983) Conversion of trifluoromethionine to a cross-linking agent by gamma-cystathionase. *Biochem. Pharmacol.* **32**, 947–950.
  55. Zygmunt, W. A. and Tavormina, P. A. (1966) DL-S-Trifluoromethylhomocysteine, a novel inhibitor of microbial growth. *Can. J. Microbiol.* **12**, 143–148.
  56. Yoshimura, M., Nakano, Y., and Koga, T. (2002) L-Methionine-gamma-lyase, as a target to inhibit malodorous bacterial growth by trifluoromethionine. *Biochem. Biophys. Res. Commun.* **292**, 964–968.
  57. Coombs, G. H. and Mottram, J. C. (2001) Trifluoromethionine, a pro-drug designed against methionine gamma-lyase-containing pathogens, has efficacy in vitro and in vivo against *Trichomonas vaginalis*. *Antimicrob. Agents. Chemother.* **45**, 1743–1745.
  58. Sato, D., Kobayashi, S., Yasui, H., Shibata, N., Toru, T., Yamamoto, M., Tokoro, G., Ali, V., Soga, T., Takeuchi, T., Suematsu, M., and Nozaki, T. Cytotoxic effect of amide derivatives of trifluoromethionine to the enteric protozoan parasite *Entamoeba histolytica*. *Int. J. Antimicrob. Agents*, in press.

59. Colombani, F., Cherest, H., and De Robichon-Szulmajster, H. (1975) Biochemical and regulatory effects of methionine analogs in *Saccharomyces cerevisiae*. *J. Bacteriol.* **122**, 375–384.
60. Duewel, H., Daub, E., Robinson, V., and Honek, J. F. (1997) Incorporation of trifluoromethionine into a phage lysozyme: implications and a new marker for use in protein  $^{19}\text{F}$  NMR. *Biochemistry* **36**, 3404–3416.
61. Ito, S., Narise, A., and Shimura, S. (2008) Identification of a methioninase inhibitor, myrsinoic acid B, from *Myrsine seguinii* Lev., and its inhibitory activities. *Biosci. Biotechnol. Biochem.* **72**, 2411–2414.
62. Hirota, M., Miyazaki, S., Minakuchi, T., Takagi, T., and Shibata, H. (2002) Myrsinoic acids B, C and F, anti-inflammatory compounds from *Myrsine seguinii*. *Biosci. Biotechnol. Biochem.* **66**, 655–659.
63. Cellarier, E., Durando, X., Vasson, M. P., Farges, M. C., Demiden, A., Maurizis, J. C., Madelmont, J. C., and Chollet, P. (2003) Methionine dependency and cancer treatment. *Cancer Treat. Rev.* **29**, 489–499.
64. Kokkinakis, D. M. (2006) Methionine-stress: a pleiotropic approach in enhancing the efficacy of chemotherapy. *Cancer Lett.* **233**, 195–207.
65. Yoshioka, T., Wada, T., Uchida, N., Maki, H., Yoshida, H., Ide, N., Kasai, H., Hojo, K., Shono, K., Maekawa, R., Yagi, S., Hoffman, R. M., and Sugita, K. (1998) Anticancer efficacy in vivo and in vitro, synergy with 5-fluorouracil, and safety of recombinant methioninase. *Cancer Res.* **58**, 2583–2587.
66. Tan, Y., Sun, X., Xu, M., Tan, X., Sasson, A., Rashidi, B., Han, Q., Tan, X., Wang, X., An, Z., Sun, F. X., and Hoffman, R. M. (1999) Efficacy of recombinant methioninase in combination with cisplatin on human colon tumors in nude mice. *Clin. Cancer Res.* **5**, 2157–2163.
67. Kokkinakis, D. M., Hoffman, R. M., Frenkel, E. P., Wick, J. B., Han, Q., Xu, M., Tan, Y., and Schold, S. C. (2001) Synergy between methionine stress and chemotherapy in the treatment of brain tumor xenografts in athymic mice. *Cancer Res.* **61**, 4017–4023.
68. Hu, J. and Cheung, N. K. (2009) Methionine depletion with recombinant methioninase: in vitro and in vivo efficacy against neuroblastoma and its synergism with chemotherapeutic drugs. *Int. J. Cancer.* **124**, 1700–1706.
69. Miki, K., Xu, M., Gupta, A., Ba, Y., Tan, Y., Al-Refai, W., Bouvet, M., Makuuchi, M., Moossa, A. R., and Hoffman, R. M. (2001) Methioninase cancer gene therapy with selenomethionine as suicide prodrug substrate. *Cancer Res.* **61**, 6805–6810.
70. Spallholz, J. E., Palace, V. P., and Reid, T. W. (2004) Methioninase and selenomethionine but not Se-methylselenocysteine generate methylselenol and superoxide in an in vitro chemiluminescent assay: implications for the nutritional carcinostatic activity of selenoamino acids. *Biochem. Pharmacol.* **67**, 547–554.
71. Yang, Z., Wang, J., Yoshioka, T., Li, B., Lu, Q., Li, S., Sun, X., Tan, Y., Yagi, S., Frenkel, E. P., and Hoffman, R. M. (2004) Pharmacokinetics, methionine depletion, and antigenicity of recombinant methioninase in primates. *Clin. Cancer Res.* **10**, 2131–2138.
72. Sun, X., Yang, Z., Li, S., Tan, Y., Zhang, N., Wang, X., Yagi, S., Yoshioka, T., Takimoto, A., Mitsushima, K., Suginaka, A., Frenkel, E. P., and Hoffman, R. M. (2003) In vivo efficacy of recombinant methioninase is enhanced by the combination of polyethylene glycol conjugation and pyridoxal 5'-phosphate supplementation. *Cancer Res.* **63**, 8377–8383.
73. Takakura, T., Takimoto, A., Notsu, Y., Yoshida, H., Ito, T., Nagatome, H., Ohno, M., Kobayashi, Y., Yoshioka, T., Inagaki, K., Yagi, S., Hoffman, R. M., and Esaki, N. (2006) Physicochemical and pharmacokinetic characterization of highly potent recombinant L-methionine gamma-lyase conjugated with polyethylene glycol as an antitumor agent. *Cancer Res.* **66**, 2807–2814.
74. Ravaglia, G., Forti, P., Maioli, F., Martelli, M., Servadei, L., Brunetti, N., Porcellini, E., and Licastro, F. (2005) Homocysteine and folate as risk factors for dementia and Alzheimer disease. *Am. J. Clin. Nutr.* **82**, 636–643.
75. Lonn, E., Yusuf, S., Arnold, M. J., Sheridan, P., Pogue, J., Micks, M., McQueen, M. J., Probstfield, J., Fodor, G., Held, C., and Genest, J. (2006) Homocysteine lowering with folic acid and B vitamins in vascular disease. *N. Engl. J. Med.* **354**, 1567–1577.
76. Bønaa, K. H., Njølstad, I., Ueland, P. M., Schirmer, H., Tverdal, A., Steigen, T., Wang, H., Nordrehaug, J. E., Arnesen, E., and Rasmussen, K. (2006) Homocysteine lowering and cardiovascular events after acute myocardial infarction. *N. Engl. J. Med.* **354**, 1578–1588.
77. Ebbing, M., Bleie, Ø., Ueland, P. M., Nordrehaug, J. E., Nilsen, D. W., Vollset, S. E., Refsum, H., Pedersen, E. K., and Nygård, O. (2008) Mortality and cardiovascular events in patients treated with homocysteine-lowering B vitamins after coronary angiography: a randomized controlled trial. *JAMA* **300**, 795–804.
78. Chan, E. C., Chang, P. Y., Wu, T. L., and Wu, J. T. (2005) Enzymatic assay of homocysteine on microtiter plates or a TECAN analyzer using crude lysate containing recombinant methionine gamma-lyase. *Ann. Clin. Lab. Sci.* **35**, 155–160.
79. Han, Q. and Hoffman, R. M. (2008) Enzymatic assay for total plasma Cys. *Nat. Protoc.* **3**, 1778–1781.
80. Han, Q., Xu, M., Tang, L., Tan, X., Tan, X., Tan, Y., and Hoffman, R. M. (2002) Homogeneous, nonradioactive, enzymatic assay for plasma pyridoxal 5-phosphate. *Clin. Chem.* **48**, 1560–1564.
81. Manukhov, I. V., Mamaeva, D. V., Rastorguev, S. M., Faleev, N. G., Morozova, E. A., Demidkina, T. V., and Zavigelsky, G. B. (2005) A gene encoding L-methionine gamma-lyase is present in enterobacteriaceae family genomes: identification and characterization of *Citrobacter freundii*-methionine gamma-lyase. *J. Bacteriol.* **187**, 3889–3893.
82. Land, K. M., Delgadillo-Correa, M. G., Tachezy, J., Vanacova, S., Hsieh, C. L., Sutak, R., and Johnson, P. J. (2004) Targeted gene replacement of a ferredoxin gene in *Trichomonas vaginalis* does not lead to metronidazole resistance. *Mol. Microbiol.* **51**, 115–122.
83. Mirelman, D., Anbar, M., and Bracha, R. (2008) Trophozoites of *Entamoeba histolytica* epigenetically silenced in several genes are virulence-attenuated. *Parasite* **15**, 266–274.

## Sensitive, Specific, and Rapid Detection of *Leishmania donovani* DNA by Loop-Mediated Isothermal Amplification

Hidekazu Takagi, Makoto Itoh,\* Mohammad Zahidul Islam, Abdur Razzaque, A. R. M. Saifuddin Ekram,  
Yoshihisa Hashighuchi, Eisei Noiri, and Eisaku Kimura

Department of Parasitology, Aichi Medical University School of Medicine, Nagakute, Aichi, Japan; Department of Medicine,  
Rajshahi Medical College Hospital, Rajshahi, Bangladesh; Department of Parasitology, Kochi Medical School, Kochi University,  
Nankoku, Kochi, Japan; Department of Nephrology and Endocrinology, and Department of Hemodialysis and Apheresis,  
University Hospital, The University of Tokyo, Tokyo, Japan

**Abstract.** We have applied a loop-mediated isothermal amplification (LAMP) technique to detect *Leishmania donovani* DNA. The LAMP technique detected 1 fg of *L. donovani* DNA, which was 10-fold more sensitive than a conventional polymerase chain reaction (PCR). All nested PCR-positive blood samples from visceral leishmaniasis patients were positive with the LAMP technique, and DNA samples from *L. infantum*, *L. major*, *L. mexicana*, *L. tropica*, *L. braziliensis*, *Plasmodium falciparum*, and healthy humans were negative with the LAMP technique. The advantages of the LAMP method are its shorter reaction time, a lack of requirement of sophisticated equipment, and visual judgment of positivity based on the turbidity of reaction mixture. Our LAMP technique can be a better alternative to a conventional PCR, especially under field conditions.

### INTRODUCTION

Visceral leishmaniasis (VL) is caused by an intracellular protozoan parasite of *Leishmania donovani* complex, and considered as one of the most neglected diseases.<sup>1</sup> Ninety percent of VL cases occur in just five countries: Bangladesh, India, Nepal, Sudan, and Brazil.<sup>2</sup> There are an estimated 500,000 new cases of VL and more than 50,000 deaths from the disease each year.<sup>3</sup> The definitive diagnosis of VL or post-kala-azar dermal leishmaniasis cases is essential for providing individual treatments and understanding the disease epidemiology. A definitive diagnosis is usually made by detecting parasites in aspirates from the spleen or other tissues (such as bone marrow, lymph nodes, or skin), parasite DNA in the tissue and blood samples, and, with lesser specificity, parasite antigen or antibody in blood or urine.<sup>4–6</sup> Although the demonstration of parasites is most specific, the techniques are invasive and require skilled personnel and proper facilities, and the sensitivity of bone marrow aspirates has been reported to be variable.<sup>4,7</sup>

In the past decade, polymerase chain reaction (PCR)-based techniques have been used more in the diagnosis of leishmaniasis.<sup>8,9</sup> To avoid invasive procedures, peripheral blood is often used, and the reported sensitivity of PCR with blood ranged from 70% to 96%.<sup>4,8–10</sup> However, PCR requires a well-established laboratory and equipment such as a thermal cycler and a system to detect and analyze amplicons.

More recently, loop-mediated isothermal amplification (LAMP) was developed as a novel method to amplify DNA with rapidity and high specificity under an isothermal condition.<sup>11,12</sup> The method consists of incubating a mixture of a target gene, four different primers, *Bst* DNA polymerase, and substrates for 1 hour at 60–65°C by using basic equipment such as a heat block or water bath. Moreover, because LAMP reactions cause turbidity in the reaction mixture proportional to the amount of amplified DNA, identification of positive or negative results is easily to make visually.<sup>13</sup> A recent report

that LAMP successfully amplified DNA of *Plasmodium falciparum* directly from heat-treated blood suggests further simplification and cost savings of the method.<sup>14</sup>

In the present study, we report a highly sensitive and specific LAMP assay to detect *L. donovani* kinetoplast DNA and its application to blood samples from patients with VL. The LAMP assay was compared with conventional and nested PCRs.

### MATERIALS AND METHODS

**Parasite DNA.** Promastigotes of *L. donovani* strain DD8, isolated from a patient in Bangladesh, were used in this study.<sup>15</sup> Promastigotes of *L. (L.) mexicana* (MNYC/BZ/62/M379), *L. (L.) major* (MHOM/SU/73/5ASKH), *L. (L.) infantum* (MHOM/TN/80/I-PT1), *L. (L.) tropica* (MHOM/SI/74/K-27), *L. (V.) braziliensis* (MHOM/BR/75/M2904), and schizont/trophozoite-rich cultured *Plasmodium falciparum* NF54 strain (kind donation by Professor Takafumi Tsuboi, Ehime University, Ehime, Japan) were also used. DNA of each species was extracted by the phenol extraction method.

**Clinical samples.** Venous blood samples were collected from 10 patients with VL confirmed by spleen biopsy at Rajshahi Medical College Hospital in Bangladesh. The blood (1 mL) was mixed with an equal volume of AL buffer (Qiagen, Valencia, CA) and kept at room temperature until it was processed at Aichi Medical University, Japan, within 1 month. DNA was extracted by using the QIAamp DNA Blood Midi Kit (Qiagen) according to the manufacturer's protocol.

This study was reviewed and approved by the Ethical Committee of Aichi Medical University School of Medicine, Japan, and the Ethical Review Committee of the Bangladesh Medical Research Council. Blood samples were collected after obtaining informed consent.

**Loop-mediated isothermal amplification.** The LAMP reaction was carried out according to the original reports described by Notomi and others<sup>11</sup> and Nagamine and others.<sup>12</sup> A set of four primers was designed specific for *L. donovani* kinetoplast minicircle DNA (GenBank accession no. Y11401) using Primer Explorer software (<http://primerexplorer.jp/>). It was not possible to design all four primers for the conserved

\* Address correspondence to Makoto Itoh, Department of Parasitology, Aichi Medical University School of Medicine, Nagakute, Aichi-gun, 480-1195, Japan. E-mail: macitoh@aichi-med-u.ac.jp

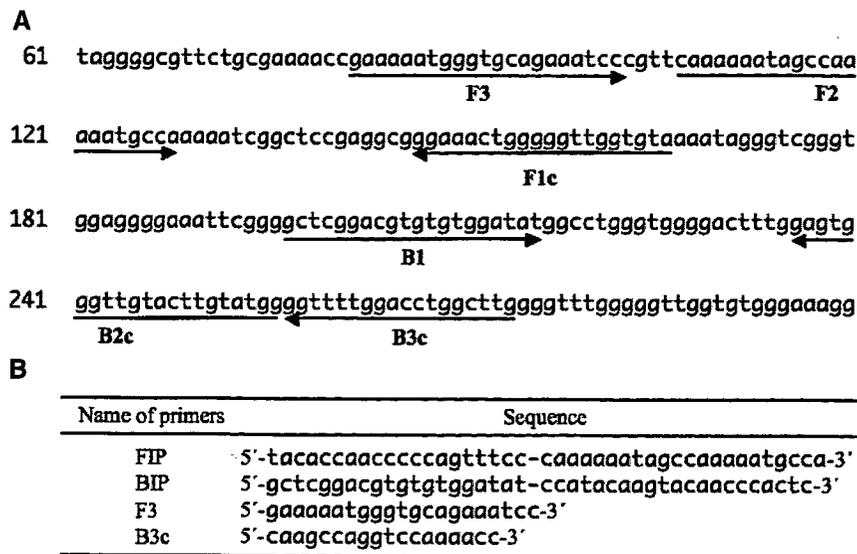


FIGURE 1. Primer set used for amplification of *Leishmania donovani* kinetoplast minicircle DNA by the loop-mediated isothermal amplification technique **A**, Locations of the primer sequences. **B**, Names and sequences of four primers. Primer FIP consists of F1 complementary sequence and F2 direct sequence. Primer BIP consists of B1 direct sequence and B2 complementary sequence.

region because of its short length; thus, two primers were designed for the variable region. The locations of targeted sequences are shown in Figure 1A.

The LAMP reaction was performed in 25  $\mu$ L of reaction mixture containing 40 pmol each of FIP and BIP primers, 5 pmol each of F3 and B3c primers, 1.4 mM of each deoxynucleoside triphosphate, 0.8 M betaine, 20 mM Tris-HCl, pH 8.8, 10 mM KCl, 10 mM  $(\text{NH}_4)_2\text{SO}_4$ , 8 mM  $\text{MgSO}_4$ , 0.1% TritonX-100, 8 units of *Bst* DNA polymerase large Fragment (New England Biolabs, Ipswich, MA), and 2  $\mu$ L of sample DNA. The mixture was incubated at 65°C for 50 minutes in a heat block. As the LAMP reaction progresses, the reaction by-product (pyrophosphate ions) binds to magnesium ions and forms a white precipitate of magnesium pyrophosphate, making the reaction fluid turbid. After incubation, the turbidity was inspected visually. For further confirmation, 3  $\mu$ L of the LAMP products was subjected to electrophoresis with a 100-basepair DNA ladder (New England Biolabs) on a 2% agarose gel and visualized under ultraviolet light after staining with ethidium bromide (5  $\mu$ g/mL).

**Conventional PCR and nested PCR.** The conventional PCR was performed according to the report of Salotra and others.<sup>16</sup> The primers used had the sequences 5'-AAATCG GCTCCGAGGCGGGAAAC-3' and 5'-GGTACTCTAT CAGTAGCAC-3'. The reaction mixture in a total volume of 50  $\mu$ L contained 10 mM Tris-HCl, pH 8.3, 50 mM KCl, 1.5 mM  $\text{MgCl}_2$ , 0.001% (w/v) gelatin, 200  $\mu$ M of each deoxynucleoside triphosphate, 0.5  $\mu$ M of each primer, and 1.25 units of AmpliTaq Gold (Applied Biosystems, Foster City, CA). The products were analyzed by electrophoresis on a 2% agarose gel in TAE buffer (40 mM Tris acetate, 1 mM EDTA). The gels were stained with ethidium bromide and photographed under ultraviolet illumination.

To augment the sensitivity and specificity, a nested PCR was performed according to the report of Sreenivas and others.<sup>17</sup> The primers used had the sequences 5'-TCGGAC GTGTGTGGATATGGC-3' and 5'-CCFATAATATAGTAT CTCCCG-3'. These primers amplified a 385-basepair frag-

ment internal to the 592-basepair product of the first PCR. The nested PCR used 1  $\mu$ L of the diluted (1:10) product from the first PCR under the same conditions as the first PCR, except for the primers.

## RESULTS

**Sensitivity of the LAMP.** A set of oligonucleotide primers designed for LAMP reaction in *L. donovani* kinetoplast DNA amplified the targeted sequences (Figure 1). To estimate the sensitivity, serially diluted *L. donovani* DNA samples containing 100 pg to 1 fg were examined. Within these concentrations, the amplification product was detected in all samples (Figure 2A and B). Conversely, with conventional PCR, the 1-fg sample was too faint to be judged positive or negative (Figure 2C, lane 6). The nested PCR showed a positive reaction in 100-pg to 1-fg samples (Figure 2D). To assess further the sensitivity of the LAMP, 20–25 aliquots of 1-fg and 100-pg DNA samples were tested. With 1 fg, 20 (80%) of 25 aliquots were positive. With 100 pg, 1 (5%) of 20 were positive. In a similar experiment using a conventional PCR, 1 (7%) of 15 test results was positive with 1 fg of parasite DNA. The nested PCR amplified 11 (55%) of 20 samples with 1 fg, but none of 20 with 100 pg. These results indicated that our LAMP was more sensitive than the nested PCR.

**Specificity of the LAMP.** To evaluate the specificity of the LAMP reaction, DNA samples from five other *Leishmania* species (*L. infantum*, *L. major*, *L. mexicana*, *L. tropica*, and *L. braziliensis*) were examined. When 100 ng of DNA was used for each *Leishmania* sample, the amplification product was not detected (Figure 3A). The same result was obtained with the nested PCR (Figure 3C). Several amplification products were detected with the conventional PCR, but they had unexpected sizes (Figure 3B, lanes 2–6). DNA from *P. falciparum* NF45 strain (100 ng) or human genomic DNA samples (500 ng each) from 11 healthy persons were also examined by LAMP; all showed negative results. These results showed that the LAMP was specific for detection of *L. donovani*.

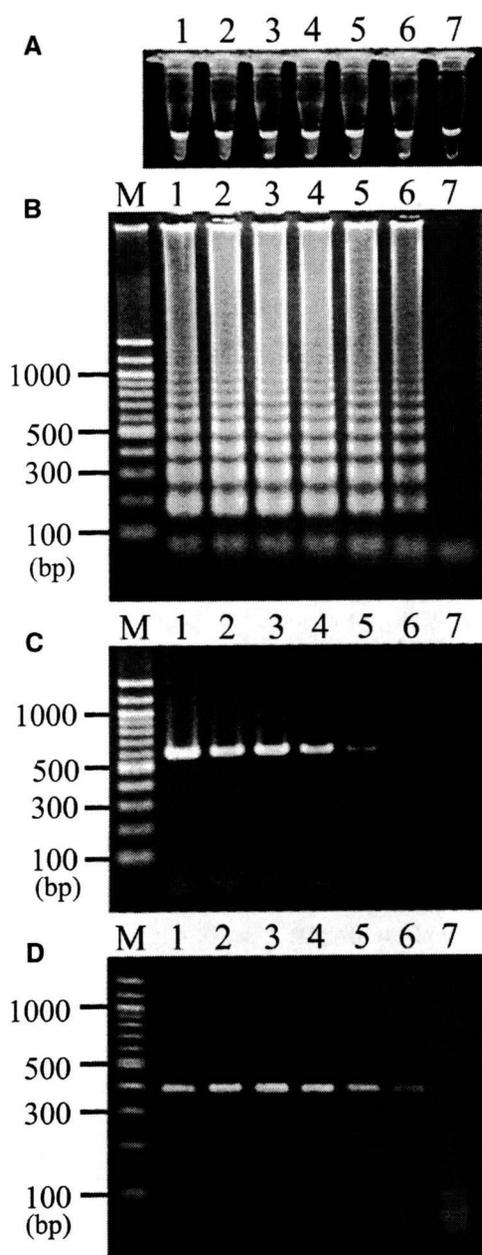


FIGURE 2. Sensitivity of loop-mediated isothermal amplification (LAMP) and polymerase chain reaction (PCR) for detection of *Leishmania donovani* DNA. **A**, Turbidity of reaction fluid produced by LAMP. **B**, Agarose gel electrophoresis of LAMP products. **C**, Conventional PCR producing a 592-basepair fragment. **D**, Nested PCR producing a 385-basepair fragment. Lane M, 100-basepair ladder; lanes 1, 2, 3, 4, 5, and 6, 100 pg, 10 pg, 1 pg, 100 fg, 10 fg, and 1 fg of DNA, respectively; lane 7, water (negative control).

**Detection of *L. donovani* DNA in blood samples from patients with VL.** Blood samples from 10 parasitologically confirmed patients with VL were examined by LAMP, conventional PCR, and nested PCR. Eight of 10 samples showed positive results with the LAMP (Figure 4A) and nested PCR (Figure 4C). Seven of the eight samples with positive results also showed positive results with the conventional PCR (Figure 4B). The DNA fragments seen in lanes 2 and N (negative control) at approximately 600 basepairs (Figure 4B) were non-specific products, which was confirmed by DNA sequencing.

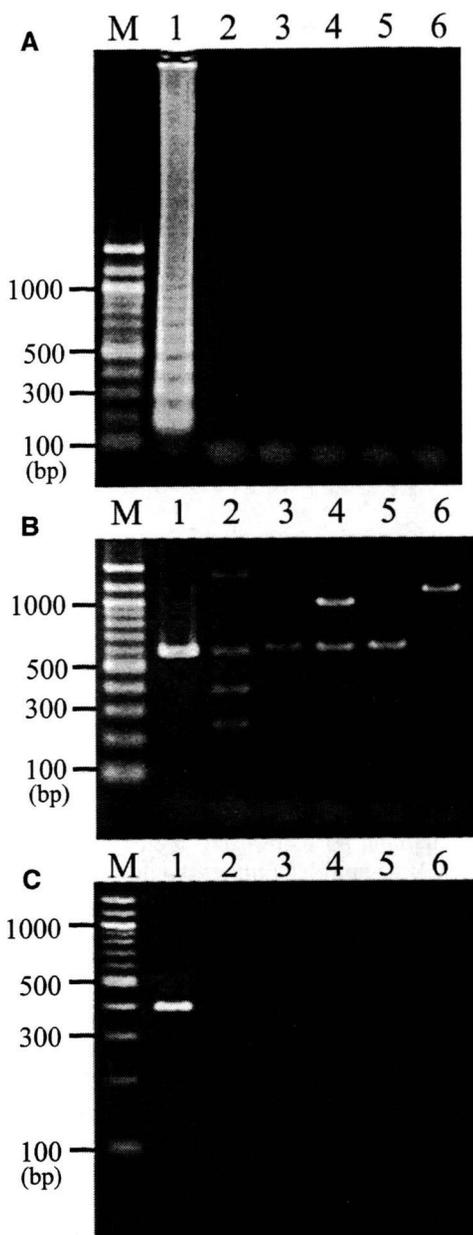


FIGURE 3. Specificity of loop-mediated isothermal amplification (LAMP) and polymerase chain reaction (PCR) for detection of *Leishmania donovani* DNA studied by agarose gel electrophoresis. **A**, LAMP. **B**, Conventional PCR. **C**, Nested PCR. Lane M, 100-basepair DNA ladder; lane 1, *L. donovani*; lane 2, *L. infantum*; lane 3, *L. major*; lane 4, *L. mexicana*; lane 5, *L. tropica*; lane 6, *L. braziliensis*.

These results indicated that the LAMP was as sensitive as the nested PCR for detecting *L. donovani* in blood samples.

#### DISCUSSION

Detection of DNA of a pathogenic agent by PCR is a definitive breakthrough in diagnosis. The LAMP assay reported by Notomi and others<sup>11</sup> is a simple and rapid DNA amplification technique based on a unique primer design and does not require a denaturation step during amplification. The new technique was applied to detect DNAs of protozoans such as *Trypanosoma* species and *P. falciparum*.<sup>14,18,19</sup> In this study, we developed a LAMP assay that could detect 1 fg of *L. donovani*

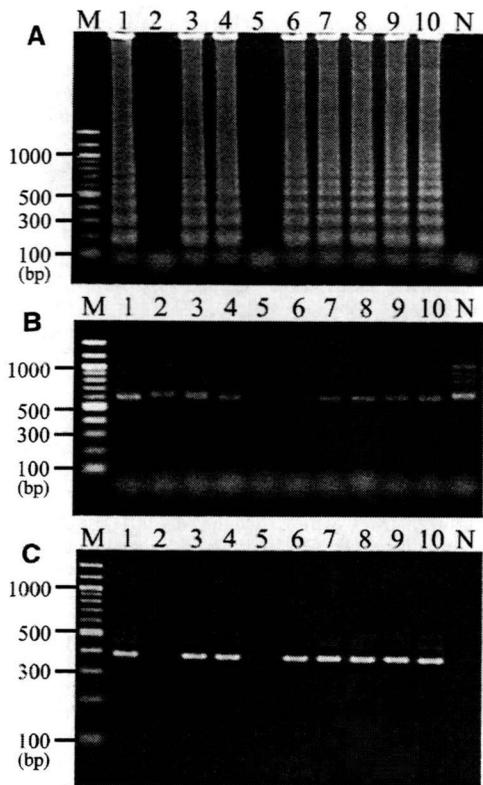


FIGURE 4. Diagnosis by loop-mediated isothermal amplification (LAMP), conventional polymerase chain reaction (PCR), and nested PCR with blood samples from confirmed patients with visceral leishmaniasis. A, LAMP. B, Conventional PCR. C, Nested PCR. Lane M, 100-basepair DNA ladder; Lanes 1–10, DNA sample from each patient; Lane N, DNA sample from a healthy human (negative control).

DNA from cultured promastigotes. The 1-fg amount is equivalent to approximately 0.1 parasites.<sup>16</sup> This high sensitivity could be achieved because of the presence of kinetoplast minicircle DNA (thousands of copies per cell).<sup>20</sup>

The specificity of LAMP is generally high because it uses four primers that recognize six locations on sample DNA.<sup>11</sup> In our study, 100 ng of DNA from each of five other species of *Leishmania* (*L. mexicana*, *L. major*, *L. infantum*, *L. tropica*, and *L. braziliensis*), 100 ng of *P. falciparum* DNA, or 500 ng of human genomic DNA all showed negative results in the LAMP assay. We designed FIP and F3 primers specific for the conserved region and BIP and B3c primers specific for the variable region of kinetoplast minicircle DNA.<sup>16,21,22</sup> Specificity for these regions might contribute further to the high specificity of the LAMP assay. However, our LAMP assay will need further confirmation with more clinical samples from different disease-endemic areas, particularly in relation to differences in *L. donovani* strains. The negative results of our PCR with *L. infantum* are in contrast to those of another report,<sup>16</sup> even though the same primer set was used (Figure 3B). Different strains of *L. infantum* used in the two studies might have some relevance to the differences observed.

Among 10 blood samples from human patients with VL confirmed by spleen biopsy, 8 (80%, 95% confidence interval = 55–100%) were positive by LAMP, and the same result was obtained by nested PCR. Although the sensitivity was not high, the present study showed comparable efficiency of the LAMP to the nested PCR, which has been generally accepted

to have much higher sensitivity than the conventional PCR.<sup>17,23</sup> Unfortunately, there is no report that evaluated the nested PCR with blood samples for the diagnosis of *L. donovani* infection.<sup>8</sup>

As for the sensitivity of the conventional PCR with blood for the diagnosis of VL, a range of 68.8% to 100% was reported in 24 papers.<sup>8</sup> The discrepancy was suggested to be caused by differences in the volume of blood used,<sup>24</sup> the stage of disease,<sup>24,25</sup> parasite species/strains,<sup>24</sup> and past treatment.<sup>24</sup> In addition, sensitivity could be influenced by immunologic status and age of the hosts and endemicity levels of their habitats.<sup>8</sup>

The presence of PCR inhibitors in a sample was also reported,<sup>26</sup> and the use of blood samples spotted on a filter paper might negatively influence results.<sup>16,27</sup> In this regard, Kaneko and others<sup>28</sup> reported that the sensitivity of LAMP was less affected by contamination with serum, plasma, or other inhibitory components in clinical samples of DNA samples than the sensitivity of the PCR.

We have developed a sensitive, urine-based, enzyme-linked immunosorbent assay (ELISA) suitable for the diagnosis of VL in the field in Bangladesh.<sup>6</sup> The LAMP could be applied to ELISA-positive urine samples to identify active infection. With a high sensitivity, LAMP would also be useful in detecting *L. donovani* DNA in skin lesions of patients suspected of having post-kala-azar dermal leishmaniasis.

Received March 18, 2009. Accepted for publication June 17, 2009.

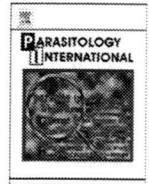
Financial support: This study was supported by the Special Coordination Funds for Promoting Science and Technology of MEXT of Japan, 1200015, and also by Grants-in-Aid for Scientific Research (B) No. 18406013 from the Japan Society for the Promotion of Science.

Authors' addresses: Hidekazu Takagi, Makoto Itoh, Mohammad Zahidul Islam, and Eisaku Kimura, Department of Parasitology, Aichi Medical University School of Medicine, Nagakute, Aichi, Japan. Abdur Razzaque and A. R. M. Saifuddin Ekram, Department of Medicine, Rajshahi Medical College Hospital, Rajshahi, Bangladesh. Yoshihisa Hashighuchi, Department of Parasitology, Kochi Medical School, Kochi University, Nankoku, Kochi, Japan. Eisei Noiri, Department of Nephrology and Endocrinology, and Department of Hemodialysis and Apheresis, University Hospital, The University of Tokyo, Tokyo, Japan.

## REFERENCES

1. Trouiller P, Olliaro P, Torreele E, Orbinski J, Laing R, Ford N, 2002. Drug development for neglected diseases: a deficient market and a public-health policy failure. *Lancet* 359: 2188–2194.
2. World Health Organization, 2002. *Wkly Epidemiol Rec* 77: 365–370.
3. Desjeux P, 2004. Leishmaniasis: current situation and new perspectives. *Comp Immunol Microbiol Infect Dis* 27: 305–318.
4. Sundar S, Rai M, 2002. Laboratory diagnosis of visceral leishmaniasis. *Clin Diagn Lab Immunol* 9: 951–958.
5. Chappuis F, Sundar S, Hailu A, Ghalib H, Rijal S, Peeling RW, Alvar J, Boelaert M, 2007. Visceral leishmaniasis: what are the needs for diagnosis, treatment and control? *Nat Rev Microbiol* 5: 873–882.
6. Islam MZ, Itoh M, Takagi H, Islam AU, Ekram AR, Rahman A, Takesue A, Hashiguchi Y, Kimura E, 2008. Enzyme-linked immunosorbent assay to detect urinary antibody against recombinant rKRP42 antigen made from *Leishmania donovani* for the diagnosis of visceral leishmaniasis. *Am J Trop Med Hyg* 79: 599–604.
7. Da Silva MR, Stewart JM, Costa CH, 2005. Sensitivity of bone marrow aspirates in the diagnosis of visceral leishmaniasis. *Am J Trop Med Hyg* 72: 811–814.

8. Antinori S, Calattini S, Longhi E, Bestetti G, Piolini R, Magni C, Orlando G, Gramiccia M, Acquaviva V, Foschi A, Corvasce S, Colomba C, Titone L, Parravicini C, Cascio A, Corbellino M, 2007. Clinical use of polymerase chain reaction performed on peripheral blood and bone marrow samples for the diagnosis and monitoring of visceral leishmaniasis in HIV-infected and HIV-uninfected patients: a single-center, 8-year experience in Italy and review of the literature. *Clin Infect Dis* 44: 1602–1610.
9. Reithinger R, Dujardin JC, 2007. Molecular diagnosis of leishmaniasis: current status and future applications. *J Clin Microbiol* 45: 21–25.
10. Singh RK, Pandey HP, Sundar S, 2006. Visceral leishmaniasis (kala-azar): challenges ahead. *Indian J Med Res* 123: 331–344.
11. Notomi T, Okayama H, Masubuchi H, Yonekawa T, Watanabe K, Amino N, Hase T, 2000. Loop-mediated isothermal amplification of DNA. *Nucleic Acids Res* 28: E63.
12. Nagamine K, Hase T, Notomi T, 2002. Accelerated reaction by loop-mediated isothermal amplification using loop primers. *Mol Cell Probes* 16: 223–229.
13. Mori Y, Nagamine K, Tomita N, Notomi T, 2001. Detection of loop-mediated isothermal amplification reaction by turbidity derived from magnesium pyrophosphate formation. *Biochem Biophys Res Commun* 289: 150–154.
14. Poon LL, Wong BW, Ma EH, Chan KH, Chow LM, Abeyewickreme W, Tangpukdee N, Yuen KY, Guan Y, Looareesuwan S, Peiris JS, 2006. Sensitive and inexpensive molecular test for falciparum malaria: detecting *Plasmodium falciparum* DNA directly from heat-treated blood by loop-mediated isothermal amplification. *Clin Chem* 52: 303–306.
15. Shamsuzzaman SM, Furuya M, Shamsuzzaman Choudhury AK, Korenaga M, Hashiguchi Y, 2000. Characterisation of Bangladeshi *Leishmania* isolated from kala-azar patients by isoenzyme electrophoresis. *Parasitol Int* 49: 139–145.
16. Salotra P, Sreenivas G, Pogue GP, Lee N, Nakhasi HL, Ramesh V, Negi NS, 2001. Development of a species-specific PCR assay for detection of *Leishmania donovani* in clinical samples from patients with kala-azar and post-kala-azar dermal leishmaniasis. *J Clin Microbiol* 39: 849–854.
17. Sreenivas G, Ansari NA, Kataria J, Salotra P, 2004. Nested PCR assay for detection of *Leishmania donovani* in slit aspirates from post-kala-azar dermal leishmaniasis lesions. *J Clin Microbiol* 42: 1777–1778.
18. Kuboki N, Inoue N, Sakurai T, Di Cello F, Grab DJ, Suzuki H, Sugimoto C, Igarashi I, 2003. Loop-mediated isothermal amplification for detection of African trypanosomes. *J Clin Microbiol* 41: 5517–5524.
19. Njiru ZK, Mikosza AS, Armstrong T, Enyaru JC, Ndung'u JM, Thompson AR, 2008. Loop-mediated isothermal amplification (LAMP) method for rapid detection of *Trypanosoma brucei rhodesiense*. *PLoS Negl Trop Dis* 2: e147.
20. Rogers WO, Wirth DF, 1987. Kinetoplast DNA minicircles: regions of extensive sequence divergence. *Proc Natl Acad Sci USA* 84: 565–569.
21. Bhattacharyya R, Das K, Sen S, Roy S, Majumder HK, 1996. Development of a genus specific primer set for detection of *Leishmania* parasites by polymerase chain reaction. *FEMS Microbiol Lett* 135: 195–200.
22. Lambson B, Smyth A, Barker D, 1999. Sequence homology within a minicircle class of the *Leishmania donovani* complex. *Mol Biochem Parasitol* 101: 229–232.
23. Gatti S, Gramegna M, Klersy C, Madama S, Bruno A, Maserati R, Bernuzzi AM, Cevini C, Scaglia M, 2004. Diagnosis of visceral leishmaniasis: the sensitivities and specificities of traditional methods and a nested PCR assay. *Ann Trop Med Parasitol* 98: 667–676.
24. Osman OF, Oskam L, Zijlstra EE, Kroon NC, Schoone GJ, Khalil ET, El-Hassan AM, Kager PA, 1997. Evaluation of PCR for diagnosis of visceral leishmaniasis. *J Clin Microbiol* 35: 2454–2457.
25. Adhya S, Chatterjee M, Hassan MQ, Mukherjee S, Sen S, 1995. Detection of *Leishmania* in the blood of early kala-azar patients with the aid of the polymerase chain reaction. *Trans R Soc Trop Med Hyg* 89: 622–624.
26. Wilson IG, 1997. Inhibition and facilitation of nucleic acid amplification. *Appl Environ Microbiol* 63: 3741–3751.
27. Maurya R, Singh RK, Kumar B, Salotra P, Rai M, Sundar S, 2005. Evaluation of PCR for diagnosis of Indian kala-azar and assessment of cure. *J Clin Microbiol* 43: 3038–3041.
28. Kaneko H, Kawana T, Fukushima E, Suzutani T, 2007. Tolerance of loop-mediated isothermal amplification to a culture medium and biological substances. *J Biochem Biophys Methods* 70: 499–501.



## Hemoglobinase activity of a cysteine protease from the ixodid tick *Haemaphysalis longicornis*<sup>☆</sup>

Kayoko Yamaji<sup>a,b</sup>, Naotoshi Tsuji<sup>b,c,\*</sup>, Takeharu Miyoshi<sup>b</sup>, M. Khyrul Islam<sup>b</sup>, Takeshi Hatta<sup>b</sup>, M. Abdul Alim<sup>b</sup>, Anisuzzaman<sup>b,c</sup>, Akio Takenaka<sup>a,d</sup>, Kozo Fujisaki<sup>e,f</sup>

<sup>a</sup> Graduate School of Life and Environmental Sciences, University of Tsukuba, Tennodai, Tsukuba, Ibaraki 305-8572, Japan

<sup>b</sup> National Institute of Animal Health, National Agriculture and Food Research Organization, Kannondai, Tsukuba, Ibaraki 305-0856, Japan

<sup>c</sup> Graduate School of Agricultural and Life Sciences, The University of Tokyo, Yayoi, Bunkyo-ku, Tokyo, 113-8657, Japan

<sup>d</sup> National Institute of Livestock and Grassland Science, National Agriculture and Food Research Organization, Ikenodai, Tsukuba, Ibaraki 305-0901, Japan

<sup>e</sup> National Research Center of Protozoan Diseases, Obihiro University of Agriculture and Veterinary Medicine, Inada-cho, Obihiro, Hokkaido 080-8555, Japan

<sup>f</sup> Department of Frontier Veterinary Medicine, Kagoshima University, Korimoto, Kagoshima 890-0065, Japan

### ARTICLE INFO

#### Article history:

Received 19 March 2009

Received in revised form 21 April 2009

Accepted 6 May 2009

Available online 13 May 2009

#### Keywords:

Tick

Cysteine protease

HICPL-A

Blood-feeding

### ABSTRACT

We report here the molecular characterization and possible function of a cysteine protease (termed HICPL-A) identified in the midgut of the hard tick *Haemaphysalis longicornis*. HICPL-A is a 333 amino acid protein belonging to the papain family of the cysteine protease. A construct encoding proHICPL-A was expressed in *Escherichia coli* and purified as both procathepsin L and active processed cathepsin L forms. The HICPL-A gene expression was up-regulated by blood-feeding process. HICPL-A exhibited substrate specificity against synthetic peptidyl substrates (Z-Phe-Arg-MCA and Z-Arg-Arg-MCA;  $k_{cat}/K_m = 0.19$  and  $0.0023 \text{ M}^{-1} \text{ S}^{-1}$ , respectively). The proteolytic activity of HICPL-A was inhibited by leupeptin, antipain and E-64 but was unaffected by pepstatin. HICPL-A was capable of degrading bovine hemoglobin at pH 3.2 to 5.6. These results suggest that HICPL-A may play important roles in the digestion of host hemoglobin in ticks.

© 2009 Elsevier Ireland Ltd. All rights reserved.

### 1. Introduction

Ticks must acquire nutrients from the host blood digestion and convert nutrients to energy [1,2]. Unlike blood-sucking insects, ticks make a blood pool by rupturing blood vessels under the host's skin and feed for a relatively long period, varying from several days to weeks, depending on the life stage, host type and the species of tick involved [3]. In ticks, blood digestion takes place slowly as an intracellular process, in contrast to that in the hematophagous insects, where protein digestion occurs rapidly in the intestinal lumen [4]. In several previous studies the midgut derived proteases with serine, cysteine, and aspartic protease activities have been described in the ixodid ticks [5–9]. Number of proteases including aspartic protease (longepsin) [10], serine carboxypeptidase (HISCP) [11] and legumain (HILgm) [12] has been ascribed to play roles in the degradation of hemoglobin (Hb) to peptides in the hard tick *Haemaphysalis longicornis*. *H. longicornis* has a wide geographical distribution in eastern Asia and Australia, and has the potential to transmit pathogens that cause important human and animal diseases [13,14]. Suppression of tick vector populations is thus crucial for con-

trolling diseases transmitted by ticks [15]. However, chemical acaricides, which are currently being used for tick control, have the disadvantages of causing acaricidal resistance problems [16], leading to food animals containing chemical residues, which are a threat to human health. Consequently, novel approaches are being sought to control tick populations based on tick-specific potential biochemical pathways.

Cysteine proteases are fundamental to almost every aspect of life cycle in hematophagous parasites, and are known to play essential roles in a wide range of biological processes, including the degradation of regulatory proteins and digestive processes [17]. One of the cysteine proteases, cathepsin L is categorized into clan CA and belongs to the cysteine protease family, C1 (cathepsin L and cathepsin B-like). Generally, cathepsin L is synthesized as a proenzyme, which is processed to a proenzyme and targeted to the lysosomes by the mannose 6-phosphate lysosomal recognition marker [18]. The proenzyme is further processed to mature forms consisting of either a single polypeptide or an active site cysteine heavy chain and a light chain linked by a disulfide bond [19]. The mature cathepsin L functions are involved in tissue remodeling, immune system, and modulation and alteration of cell function [20]. In contrast to most members of the C1A subfamily, which commonly have a neutral pH optimum, cathepsin L has an acidic pH optimum, and their activity would be maximal in the acidic environment of the lysosome [17]. In a variety of hematophagous endo- and ectoparasites [21,22], cathepsin L takes part in nutrient acquisition by catabolizing host Hb to peptides.

<sup>☆</sup> Nucleotide sequences data reported in this paper will appear in the EMBL, GenBank and DDBJ databases under the accession numbers AB490783.

\* Corresponding author. Laboratory of Parasitic Diseases, National Institute of Animal Health, 3-1-5, Kannondai, Tsukuba, Ibaraki 305-0856, Japan. Tel./fax: +81 29 838 7749. E-mail address: [tsujin@affrc.go.jp](mailto:tsujin@affrc.go.jp) (N. Tsuji).

We describe here the functional characterization of a cDNA encoding a cysteine protease from the hard tick *H. longicornis* (HICPL-A), whose amino acid sequence shows similarity with mammalian cathepsin L sequences. HICPL-A gene expression was up-regulated by blood-feeding process. HICPL-A hydrolyzed not only synthetic peptide substrates for cathepsin L/B, but also the natural substrate bovine Hb. Our results strongly suggest that HICPL-A plays a key role in the digestion of host Hb by *H. longicornis*.

## 2. Materials and methods

### 2.1. Ticks and animals

*H. longicornis* (Okayama strain) were maintained at the Laboratory of Parasitic Diseases, National Institute of Animal Health, Tsukuba, Ibaraki, Japan, on rabbits as described previously [23]. All animals used this study were acclimatized to the experimental conditions for 2 weeks prior to the experiment. Animal experiments at the National Institute of Animal Health were conducted in accordance with protocols approved by the Animal Care and Use Committee, National Institute of Animal Health (Approval nos. 08-021).

### 2.2. Cloning and sequencing of HICPL-A

HICPL-A was identified from ESTs constructed from midgut cDNA libraries of *H. longicornis* as described previously [10]. The plasmids containing HICPL-A gene-encoding inserts were extracted using the Qiagen DNA Purification kit (QIAGEN Sciences, Germantown, MA, USA). The nucleotide sequences of the cDNAs were determined by the BigDye Terminator method on an ABI PRISM 3100 automated sequencer (Applied Biosystems, Foster City, CA, USA). The GENETYX-WIN DNA analysis software system (Software Inc.) was used to deduce the amino acid sequence of HICPL-A. Alignments of protein sequences within other homologues were performed at the DNA Data Bank of Japan (<http://blast.ddbj.nig.ac.jp/top-j.html>). Signal peptide analysis was performed using the SignalP version 3.0 (<http://www.cbs.dtu.dk/services/SignalP>) program [24].

### 2.3. Quantitative reverse transcription (RT-PCR)

Total RNA was extracted from the midgut and salivary gland of adult ticks with RNeasy Mini Kit (QIAGEN) following the manufacturer's instructions. cDNA synthesis from total RNA was performed with a Takara RNA PCR Kit (AMV) Ver3.0 (Takara Bio Inc., Otsu, Japan). The primers combination was as follows: 5' GCAGCACAATAAGGCG-TACA 3' (forward primer), 5' GACCATTTGGCGAACTCAT 3' (reverse primer) for HICPL-A. Transcript abundance was measured with a LightCycler 1.5 (Roche Instrument Center AG, Roikreuz, Switzerland) according to the manufacturer's instructions. Quantitative RT-PCR was conducted in LightCycler Capillaries (Roche) with a 20 µl reaction volume containing 4.6 µl of LightCycler FastStart DNA Master SYBR Green (Roche), 3 mM of MgCl<sub>2</sub>, 0.5 µM of each forward and reverse primer, and cDNA corresponding to 0.2 ng of total RNA. Expression was normalized against β-actin as internal control. The mRNA abundance unit was calculated as the number of mRNA molecules per β-actin mRNA. The data were analyzed by LightCycler Software Version 3.5. The β-actin gene was amplified according to the same procedures and used as a control. Each analysis was done at least in triplicate.

### 2.4. Expression and purification of recombinant proHICPL-A from *Escherichia coli*

The cDNA fragments spanning the whole HICPL-A open reading frame (ORF), devoid of their signal peptide sequence, were amplified by PCR with AmpliTaq Gold DNA polymerase (Applied Biosystems) and

appropriate oligonucleotide primers, forward: 5' CCGGAATTCGGCAA-GAAATCCTCCGTACCG 3', reverse: 5' CCGCTCGAGCGGCTAAACAAGTGG-GTAGCTTG 3', which contained a EcoRI and a XhoI enzyme restriction site (as indicated by underline). PCR conditions were: 30 s at 95 °C, 30 s at 55 °C and 2 min at 72 °C for 35 cycles. A final 5 min extension was performed at 72 °C. The PCR product was inserted in the frame into the fusion expression vector pGEX-6p-1 (GE Healthcare Bio-Sciences AB, Piscataway, NJ). *E. coli* BL21 (Invitrogen, Carlsbad, CA) containing the recombinant plasmids were grown in SOB medium at 37 °C to an OD<sub>550</sub> of c. 0.5 and induced with 1 mM IPTG (isopropyl β-D-thiogalactopyranoside) for 6 h. Bacterial cells overexpressing the proHICPL-A were harvested and processed as described previously [25]. The fusion proteins with a GST tag were purified using a Glutathione Sepharose 4B (GE Healthcare) following the manufacturer's instructions and then cleaved with PreScission Protease (GE Healthcare), and purification was checked by sodium dodecyl sulfate polyacrylamide gel electrophoresis (SDS-PAGE). Total protein concentration was determined by BCA Protein Assay Kit (Thermo Electron Corporation, Waltham, MA, USA).

### 2.5. Purification of heterogeneous HICPL-A

The mature HICPL-A was generated by incubating the purified proHICPL-A at 37 °C for 1 h in citrate–sodium phosphate buffer (pH 3.6) containing 1 mM DTT. After this activation process, recombinant products were dialyzed against the Tris–HCl buffer (20 mM Tris–HCl, pH 7.4, 150 mM NaCl). Purity of the fractions was checked by SDS-PAGE.

### 2.6. Enzymatic activity of HICPL-A

To detect the hydrolysis efficiency of HICPL-A, we employed fluorogenic peptidyl substrates suitable for quantifying cysteine protease activity. The substrates were benzyloxycarbonyl-L-phenylalanyl-L-arginine-4-methylcoumaryl-7-amide (Z-Phe-Arg-MCA) to measure cathepsin B/L activities and benzyloxycarbonyl-L-arginyl-L-arginine-4-methylcoumaryl-7-amide (Z-Arg-Arg-MCA), which is selective for cathepsin B. The synthetic substrates Z-Phe-Arg-MCA and Z-Arg-Arg-MCA were purchased from Peptide Institute Inc, Osaka, Japan. HICPL-A (0.1 µM) was preincubated for 30 min in assay buffer (100 mM NaAc, pH 5.5, 100 mM NaCl, 1 mM EDTA, 1 mg/ml cysteine, and 0.005% TritonX-100) at 37 °C. Fluorogenic peptidyl substrates were added to have a final concentration of 0.25 mM. Fluorogenic assays were monitored by fluorescence spectrophotometry at 380 nm excitation and 460 nm emission (TECAN, Maennedorf, Switzerland). For substrates,  $K_m$  and  $k_{cat}$  values were obtained by fitting the initial rates to the Michaelis–Menten equation using nonlinear regression analysis (Graph Pad 4.0, CA, USA).

The optimum pH for the enzyme activity was determined using citrate–sodium phosphate buffer with a pH range of 3.6–8.0 and the optimum temperature was determined using citrate–sodium phosphate buffer with a pH of 5.5. The ability of protease inhibitors, antipain (inhibitor for trypsin, u-PA, papain and cathepsin A/B), E-64 (inhibitor for thiol proteases), pepstatin A (inhibitor for pepsin, cathepsin D/E and renin), leupeptin (inhibitor for trypsin, plasmin, papain and cathepsin B), to inhibit HICPL-A activity against each substrate was also investigated. HICPL-A (0.1 µM) was preincubated with different concentrations of inhibitor for 30 min in assay buffer (100 mM NaAc, pH 5.5, 100 mM NaCl, 1 mM EDTA, 1 mg/ml cysteine, and 0.005% TritonX-100) at 37 °C. Fluorogenic peptidyl substrates were added to five a final concentration of 0.2 mM.

### 2.7. HICPL-A hydrolyzes Hb

HICPL-A was incubated in the presence of bovine Hb (Sigma, St. Louis, MO) in a total volume of 5 µg at 37 °C. To monitor the effect of pH on the activity of the HICPL-A (1 µg), the assay was performed using citrate–sodium phosphate buffer with pH values ranging from

3.2 to 8.0. Incubation time and concentration assay were performed with Hb (5 µg) in citrate–sodium phosphate buffer (pH 3.6). Cleavage products were resolved by SDS-PAGE using 10–20% Tricine gel (Invitrogen). Gels were stained with Coomassie Brilliant Blue.

**3. Results**

**3.1. Identification and characterization of HICPL-A, a cathepsin L-like homologue in *H. longicornis***

HICPL-A was identified from ESTs constructed from midgut cDNA libraries of *H. longicornis* as described previously [10]. The cDNA encoding the gene product was amplified from *H. longicornis* RNA by RT-PCR, subcloned, and sequenced. The 1002-bp cDNA encoded a cathepsin L-like protease, proHICPL-A, having 333 amino acids with a predicted molecular weight (MW) of 36,271.65 and an isoelectric point (pI) of 6.45. The cleavage site of the signal sequence was predicted to be between S<sup>19</sup> and Q<sup>20</sup> (HICPL-A ORF numbering). The proHICPL-A cleavage site was predicted between S<sup>116</sup> and L<sup>117</sup> based on the N-terminal sequence information from the cathepsin L of human, bovine and rat (Fig. 1) [26]. The HICPL-A ORF contained each of the conserved motifs identified in the active site of lysosomal cathepsins including the residues that form the catalytic triad, C<sup>141</sup>, H<sup>279</sup> and N<sup>299</sup>

H-A	1	---	MLRLAFLQCGVAAIAAASSQEILRTEWEAFKSNHNKAYS	SHVEELLR
Ir	1	---	MLRCLVLCVLLVAAAAVSVYQEVLGAEWSAFKAKHGKSYVSETEVFR	
Bm	1	---	MLRSLVLCVCAIVAVTVAASSQEILRTQWEAFKTHHKSYQSHMEELLR	
Hs	1	MNPTLL	LAAFCVLCGASATLT-FDHSLEAQWTKWKAMHNRLYG-MNEEGWR	
Rn	1	MTPDLLL	LAVALCLGSLATLTPK-FDQTFNAQWHQWKSTHRRLYG-TNEEWR	
H-A	48	FKIFTENTLL	VAKHNKAKYAGLVSYKLANMKFGDLLPHEFAKMNVGYSR--	
Ir	48	LKIYENRHHKIAKHNK	YARGEVVPYSMANNEFGDMLHHEFVSTRNGFKRN	
Bm	48	FKIFTENSLI	IAKHNKAKYAGLVSYKLGNNQFGDLLAHEFARIFNGHH--	
Hs	49	RAVWEKNMKMIELHNQ	YREGKHSFTMAMNAPFGDMTSEEFQVMNGFQ--	
Rn	49	RAVWEKNMRMIQLHNG	YSEYSGKHGFTMEMNAPFGDMTNEEFQIVNGYSR--	
H-A	96	GKQNK	QQRFTFIPANLNDSSLPTTVDWRKKGAVTPVKNGQCGGSAWAFS	
Ir	98	YKDQ	PREGSTYLEPENIEDPSLPKTVDRWTKGAVTPVKNGQCGGSAWAFS	
Bm	96	GTR-KTGG	SFTLPPANVNDSSLPKVVDWRKKGAVTPVKNGQCGGSAWAFS	
Hs	96	-NRKPRK	GVFQEPFLFYE--APRSVDWREKGYVTPVKNGQCGGSAWAFS	
Rn	96	-HQKHK	KGRFLQEPFLMLQ---IPKTVDRWREKGCVTPVKNGQCGGSAWAFS	
H-A	146	TTGSL	EGQHFRKTKGLVSLSEQNLVDCSDDFGNQGCNGGLMDNGFQYIKA	
Ir	148	ATGSL	EGQHFRKSGSMVLSLSEQNLVGCSTDFGNNGCEGGLMDDAFKYIRA	
Bm	145	ATGSL	EGQHFLKNGELVSLSEQNLVDCSQSPGNNGCEGGLMEDAFKYIKA	
Hs	143	ATGALE	GQMFRTGRLISLSEQNLVDCSGPQGNBGCNGGLMDYAFQYVQD	
Rn	143	ASGCLE	GQMFRLTKGLISLSEQNLVDCSHDQGNQGCNGGLMDFAFQYIKE	
H-A	196	NGGID	TEESHPTYAQDGDCKFKKADVVGATDAGFVDIQQGS	EDDLKKA
Ir	198	NKGID	TEKSYYPYNGTDGTCFKKSTVGATDSTGDFDIKEGSETQLKKA	
Bm	195	NDGID	TEKSYYPYEAVDGECRFKEDVVGATDTGYVEIKAGSEVDLKKA	
Hs	193	NGGLD	EESYPYEAATEESCKYNPKYSVANDTGFVDIPQ-QEKALMKA	
Rn	193	NGGLD	EESYPYEAADGSCYRAEYAVANDTGFVDIPQ-QEKALMKA	
H-A	246	VGPVS	VAIDASHGFSQLYSGVYDEPDCSSQLDGLVTVGYGVK----	N
Ir	248	VGPI	SVAIDASHESFQFYSQVYDEPCDSESLDGLVTVGYGTL----	N
Bm	245	VGPI	SVAIDASHESFQLYSEGVYDEPCDSESLDGLVTVGYGVK----	G
Hs	242	VGPI	SVAIDAGHESFLFYKGIYFRPDCSSRDMDGLVTVGYGFSTESD	
Rn	242	VGPI	SVAIDASHPSLQFYSSGIYFEPNCSSKDLGLVTVGYGEGTDSN	
H-A	292	GKKY	WLVKNSWGGDWDGNGYILMSRDKDNQCGIASSASYPLV-	
Ir	294	GTDY	WVFNKSWGTTWGDGEGYIEMSRNKNQCGIASSASYPLV-	
Bm	291	GKKY	WLVKNSWAEWGDQGYILMSRDNNQCGIASSQASYPLV-	
Hs	292	NNKY	WLVKNSWGEWGMGGYVKMAKDRRNHCGIASSASYPTV-	
Rn	292	KDKY	WLVKNSWGEWGMGGYIKIAKDRRNHCGIASSASYPTV-	

**Fig. 1.** Comparison of conserved regions in the amino acid sequences of the cysteine proteinase identified from *H. longicornis* (HICPL-A) and those from mammals and arthropods. *Ixodes ricinus* (Gen Bank accession no. ABO26562); *Rattus norvegicus* (AAH63175); *Homo sapiens* (AAA66974); *Boophilus microplus* (AAF61565). Conserved active site residues are shown in box. Identical residues are marked with asterisks. The square dots indicate the papain-like cysteine protease conserved motif. Arrows indicate the cleavage sites. H-A, HICPL-A; Ir, (*I. ricinus*); Rn, (*R. norvegicus*); Hs, (*H. sapiens*); Bm, (*B. microplus*).

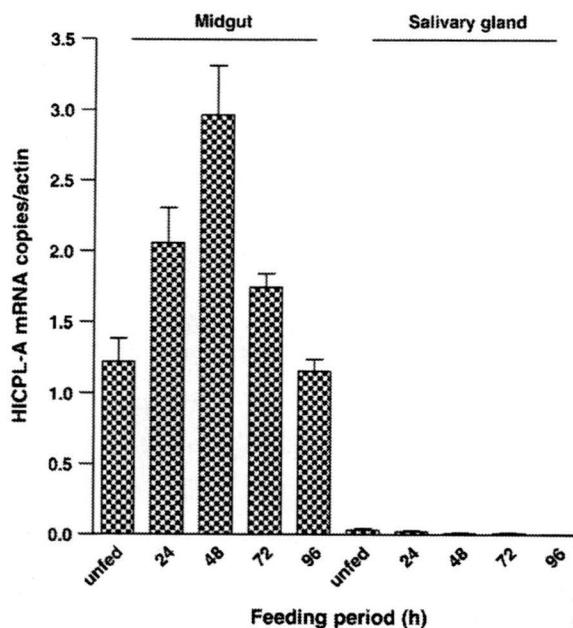


**Fig. 2.** Quantitative RT-PCR analysis of HICPL-A regulation at different stages of blood-feeding. Quantitative RT-PCR was performed on total RNA extracted from *H. longicornis* at different stages. The bars show the mean ± SD of relative mRNA copy numbers (n = 4).

(Fig. 1B, boxed residues). The calculated MW of the mature protein, HICPL-A, is 23,185.52 with pI 4.89.

**3.2. Expression of HICPL-A is induced by the blood-feeding process**

To examine the expression of HICPL-A in midgut and salivary gland during the blood-feeding process, we performed quantitative RT-PCR with total RNA extracted from the unfed and partially fed (24, 48, 72 and 96 h) adult ticks. We found that HICPL-A was expressed in the midgut and salivary gland. In the midgut, HICPL-A mRNA was expressed in both unfed and partially fed ticks. The mRNA expression was increased on blood-feeding which reached to its peak at 48 h of feeding and there

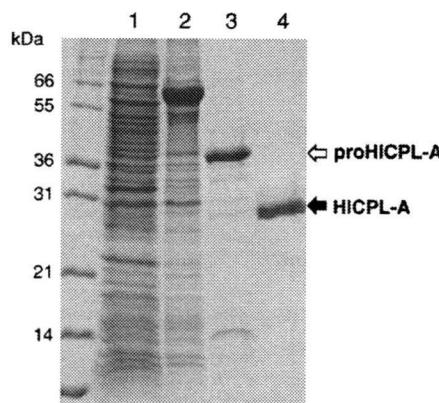


**Fig. 3.** Purification of recombinant proHICPL-A and processed HICPL-A from *E. coli*. Protein samples were subjected to 12.5% SDS-PAGE under reducing conditions and stained with Coomassie Brilliant Blue. Lane 1, 5 µg of crude lysate of *E. coli* before induction. Lane 2, 5 µg of crude lysate of *E. coli* incubated with 0.1 mM IPTG for 6 h. Lane 3, 5 µg of purified recombinant proHICPL-A. Lane 4, 5 µg of purified HICPL-A. The white arrowhead indicates recombinant proHICPL-A, and the black one indicates recombinant HICPL-A. Positions and sizes of marker proteins are indicated on the left.

after gradually decreased. The mRNA expression, however, was in very negligible level in adult tick salivary glands (Fig. 2).

### 3.3. Autoactivation of the purified recombinant HICPL-A

HICPL-A was expressed in *E. coli* using a gene expression system based on inducible pGEX-6P-1. The fusion proteins with a GST tag were purified using a Glutathione Sepharose 4B. Preliminary tests revealed that HICPL-A remains stable as the zymogen at pH 7.6, but undergoes autoactivation at pH 3.6. The purified enzyme is initially present as the 38 kDa proform. Processing was completed by 1 h of incubation, with the conversion of the proform to the 29 kDa mature enzyme form (Fig. 3). Autocatalytic processing of the precursor to the mature enzyme form by the removal of the NH<sub>2</sub>-terminal propeptide has also been reported for the cysteine endopeptidases papain and cathepsin L under similar conditions [27,28].

### 3.4. HICPL-A cleaves fluorogenic peptidyl substrates

We performed assay to detect the hydrolysis efficiency of HICPL-A, by employing fluorogenic peptidyl substrates suitable for quantifying cysteine protease activity. Activity was determined with the substrates Z-Phe-Arg-MCA and Z-Arg-Arg-MCA. Initial studies showed that the enzyme efficiently cleaved Z-Phe-Arg-MCA (cathepsin L and cathepsin B specific substrate) and Z-Arg-Arg-MCA (cathepsin B specific substrate) but exhibited minimal activity against Z-Arg-MCA, a substrate diagnostic of cathepsin H (data not shown). HICPL-A exhibited much higher activity toward Z-Phe-Arg-MCA, however, notably, it had little activity on Z-Arg-Arg-MCA (Table 1). These results suggest that HICPL-A is a cysteine protease of cathepsin L activities.

### 3.5. pH and temperature dependency of HICPL-A

The cathepsin B/L fluorogenic substrate Z-Phe-Arg-MCA was used to determine the effects of pH and temperature on the activities of HICPL-A. We determined the pH optima of HICPL-A and proHICPL-A activities between pH 2.8 and 8.0. Optimal hydrolysis was measured at acidic pH at 3.6 (Fig. 4A). No substantial hydrolysis of substrate occurred at above pH 6.0. With increasing temperature, the activity was enhanced, reaching the maximum at 40 °C for Z-Phe-Arg-MCA substrate hydrolysis (Fig. 4B).

### 3.6. Inhibition of HICPL-A activity

Protease inhibitors were tested to inhibit the activity of HICPL-A by using the substrate Z-Phe-Arg-MCA (Fig. 5). The proteolytic activity of HICPL-A was inhibited by E-64, antipain and leupeptin but was unaffected by pepstatin, indicating that HICPL-A is a cysteine protease.

### 3.7. HICPL-A proteolyses Hb

To assess the proteolysis efficiency of HICPL-A, bovine Hb was incubated with HICPL-A for 1 h and was subjected to SDS-PAGE analysis. As shown in Fig. 6A, HICPL-A was found to degrade Hb in a dose-dependent manner at pH 5.5 and at a temperature of 37 °C. We observed that under acidic conditions (pH 3.2–5.6), HICPL-A rapidly

**Table 1**  
Kinetic constants for hydrolysis of substrates.

Substrates	$K_m$ ( $\mu\text{M}$ )	$k_{\text{cat}}$ ( $\text{s}^{-1}$ )	$k_{\text{cat}}/K_m$ ( $\text{m}^{-1}\text{s}^{-1}$ )
Z-Phe-Arg-MCA (substrate for cathepsin L/B)	$40.78 \pm 4.307$	7.868	0.19
Z-Arg-Arg-MCA (substrate for cathepsin B)	$54.77 \pm 11.14$	0.126	0.0023

HICPL-A (0.1  $\mu\text{M}$ ) was incubated in assay buffer (100 mM NaAc, pH 5.5, 100 mM NaCl, 1 mM EDTA, 1 mg/ml cysteine, and 0.005% TritonX-100) with 0.25 mM of the substrates at 37 °C.

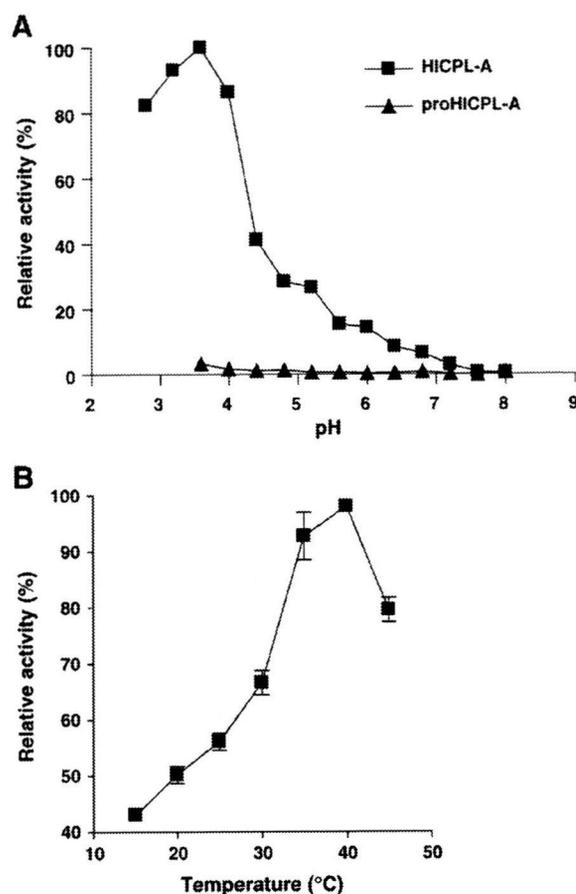


**Fig. 4.** (A) Recombinant proHICPL-A and processed HICPL-A pH stability. Enzyme samples were preincubated for 30 min at 37 °C in a range of buffer (pH 2.8–8.0). Activity remaining was assayed at pH 5.5 with the substrate Z-Phe-Arg-MCA.  $\blacktriangle$ , proHICPL-A.  $\blacksquare$ , HICPL-A. (B) Effect of temperature on recombinant HICPL-A activity at pH 5.5. Data are expressed as the mean percent enzyme activity relative to the maximum activity  $\pm$  SD ( $n=4$ ).

degrades bovine Hb into low-molecular weight fragments (Fig. 6B). Moreover, HICPL-A was found to degrade Hb after 10 min of incubation at 37 °C (Fig. 6C).

## 4. Discussion

The elucidation of digestive processes in the ticks' guts that leads to the utilization of the blood-meal will result in a deeper understanding of the physiology of blood digestion. However, the molecular basis of how the digestion is maintained in nature during the complex life cycle of ticks, is poorly understood. The full length transcript of HICPL-A encodes a proHICPL-A of 333 amino acid residues, which includes a signal peptide. HICPL-A has shown to conserve catalytic triad, Cys-141, His-279, and Asn-299 (HICPL-A numbering), which is indispensable for enzyme activity and there are highly conserved regions among mammalian and arthropod cysteine proteases. Moreover, the protease was processed post-translationally to the mature active form. We have shown that proHICPL-A can be expressed at high levels in *E. coli* and the purified proenzyme was of 38 kDa. After post-translational processing, the mature enzyme was with an apparent molecular mass of 29 kDa. Either secreted or lysosomal enzymes of the papain family are synthesized with signal peptides. Lysosomal cysteine proteases, generally known as the cathepsins, are synthesized as inactive precursors, and are activated by proteolytic removal of the N-terminal propeptide [26]. It has also been reported that to protect

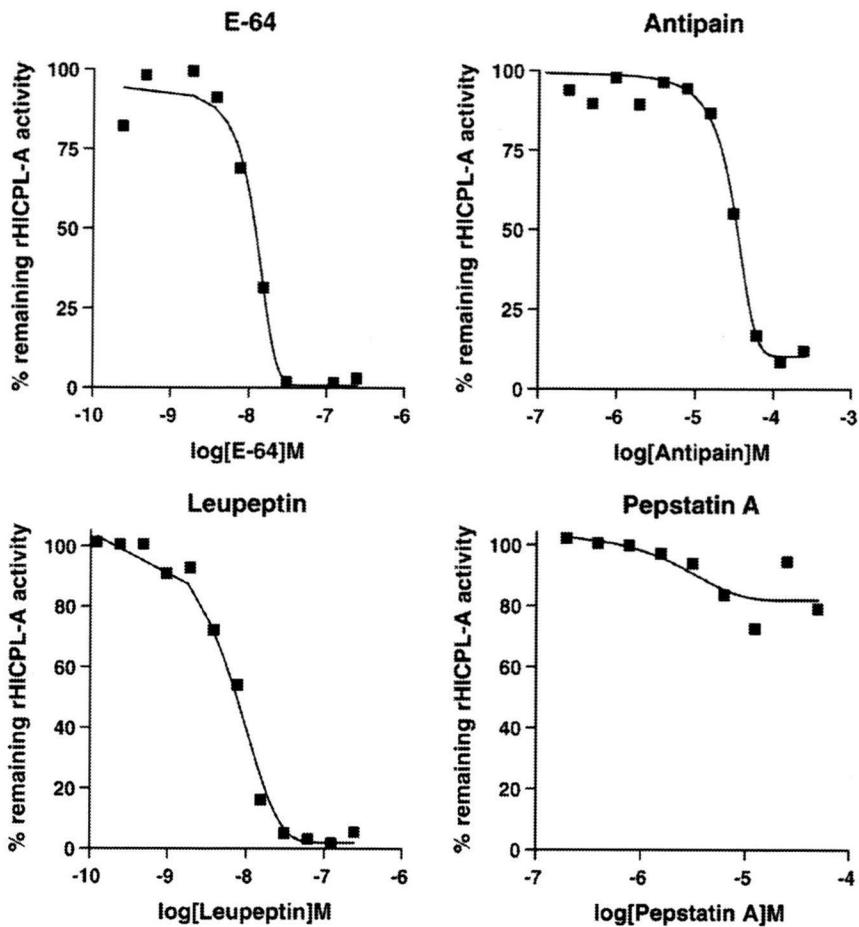


Fig. 5. Inhibition of HICPL-A enzyme activity toward Z-Phe-Arg-MCA and Z-Arg-Arg-MCA by proteinase inhibitors. HICPL-A (0.1  $\mu$ M) was incubated in assay buffer (100 mM NaAc, pH 5.5, 100 mM NaCl, 1 mM EDTA, 1 mg/ml cysteine, and 0.005% TritonX-100) at 37 °C with the protease inhibitors.

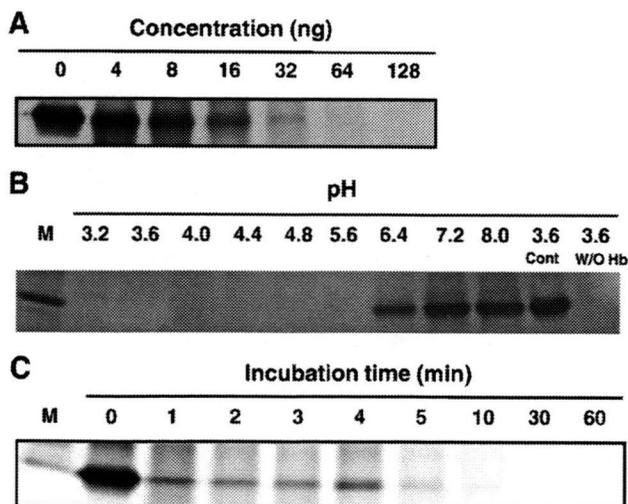


Fig. 6. HICPL-A proteolyses Hb. Effect of concentration (A), pH (B) and incubation time (C) on Hb degradation by HICPL-A. (A,C) Bovine Hb (5  $\mu$ g) was incubated in assay buffer (100 mM NaAc, pH 5.5, 100 mM NaCl, 1 mM EDTA, 1 mg/ml cysteine, and 0.005% TritonX-100) with HICPL-A at 37 °C. (B) Hb (5  $\mu$ g) was incubated with HICPL-A (1  $\mu$ g) in citrate-sodium phosphate buffer with a pH range of 3.2–8.0 at 37 °C. Cont, reaction buffer containing bovine Hb without the addition of HICPL-A and incubators. M, marker proteins (14 kDa).

cells from the potentially disastrous consequences of uncontrolled degradative activity, essentially all known cellular proteolytic enzymes are synthesized as inactive precursors [29]. The removal of ~11 kDa N-terminal propeptide from proHICPL-A that resulted in mature HICPL-A was autocatalytic, as is the case with other papain family proteases, including papain [30], cathepsin B [31], cathepsin L [32], and cathepsin K [33].

In this study, we examined the cysteine protease activity in HICPL-A using class-specific, synthetic peptidyl substrates that could discriminate between classes of papain-like cysteine proteases, namely cathepsin L, cathepsin B, and cathepsin H. HICPL-A exhibited potent hydrolytic activity on Z-Phe-Arg-MCA (substrate for cathepsin L/B), while it showed little activity towards Z-Arg-Arg-MCA (substrate for cathepsin B), and very minimum activity was achieved with Z-Arg-MCA (substrates for cathepsin H). Moreover, proteolytic activity of the HICPL-A was inhibited by cysteine- and serine-proteinases inhibitors such as E-64, antipain and leupeptin but was unaffected by aspartic proteinase inhibitor (pepstatin). The substrate specificity and inhibitor sensitivity indicate that HICPL-A is a typical cathepsin L.

The expression of *HICPL-A* gene was found to be up-regulated by the blood-feeding process. HICPL-A showed pH optima at pH 3.6 for activity against synthetic peptidyl substrates and bovine Hb. Generally, lysosomal cysteine proteases are optimally active in the acidic, lysosomal environmental [26]. The optimum pH of the enzyme involved in intracellular digestion is thought to be around 3.0 [34], which is suitable to act in acidic environment of lysosomes. The presence of aspartic and cysteine proteinases proteolytic activities has been indicated in the midgut of *Boophilus microplus* [35]. A few physiological studies have

revealed that the digestive activity of ixodids becomes high at the middle of the feeding stage [36]. The transcriptional profile and the peptidyl substrates including Hb degradation suggest that HICPL-A is involved in the blood digestion within the lysosomes during the blood-feeding process.

The major food source of blood-feeding parasites, Hb, is degraded by a cascade of proteases in the intestine that cleave the intact Hb tetramer into successively smaller fragments. In the malaria parasites *Plasmodium*, an ordered pathway of Hb digestion has been revealed and includes members of cysteine and aspartic proteases [37,38]. The present finding also strongly suggests the involvement of midgut cysteine protease in Hb digestion pathway in the ixodid ticks [39].

Further elucidation of the functional properties of HICPL-A will help in evaluating the enzyme as a drug target or vaccine candidate for the purpose of better control of ticks and tick-borne diseases. Our results obtained in the present study demonstrate that HICPL-A expressed by midgut appears to play key roles in the digestion of host Hb, the principal source of amino acid nutrients utilized by ticks. The distinctive life-cycle pattern and feeding behaviour of ticks has led to the evolution of unique molecular mechanisms which differ from those in mammalian hosts. Tick proteolytic enzymes in the midgut may be useful for controlling ticks through vaccination [40,41]. Elucidating the biological roles of these proteases and attaining a thorough knowledge of their biochemistry and structure are required for designing tick vaccine antigens which specifically block proteolytic action and thereby interfere with tick survival and reproduction.

#### Acknowledgements

This work was supported by Grant-in-Aids (to N.T. and K.F.) from the Ministry of Education, Culture, Sports, Science, and Technology of Japan. This work was also supported by a grant (to N.T. and K.F.) for Promotion of Basic Research Activities for Innovative Biosciences from the Bio-oriented Technology Research Advancement Institution.

#### References

- [1] Smit JD, Grandjean O, Guggenheim R, Winterhalter KH. Haemoglobin crystals in the midgut of the tick *Ornithodoros moubata* Murray. *Nature* 1977;266:536–8.
- [2] Braz GR, Coelho HS, Masuda H, Oliveira-PL. A missing metabolic pathway in the cattle tick *Boophilus microplus*. *Curr Biol* 1999;9:703–6.
- [3] Klompen H. Ticks, the Ixodida. *Biology of Disease Vectors*. 2nd ed. Elsevier Academic Press; 2005. p. 45–55. (Marquardt WC, edn.).
- [4] Coons LB, Rosell-Davis R, Tamowski BI. Blood meal digestion in ticks. In: Sauer JR, Hair JA, editors. *Morphology, Physiology and Behavioural Biology of Ticks*. Ellis Harwood, Wiley, New York; 1986. pp. 248–279.
- [5] Miyoshi T, Tsuji N, Islam MK, Alim MA, Hatta T, Huang X, et al. A set of serine proteinase paralogs are required for blood-digestion in the ixodid tick *Haemaphysalis longicornis*. *Parasitol Int* 2008;57:499–505.
- [6] Mulenga A, Sugimoto C, Onuma M. Characterization of proteolytic enzymes expressed in the midgut of *Haemaphysalis longicornis*. *Jpn J Vet Res* 1999;46:179–84.
- [7] Sojka D, Franta Z, Horn M, Hajdusek O, Caffrey CR, Mares M, et al. Profiling of proteolytic enzymes in the gut of the tick *Ixodes ricinus* reveals an evolutionarily conserved network of aspartic and cysteine peptidases. *Parasitol Vectors* 2008;1:7.
- [8] Renard G, Garcia JF, Cardoso FC, Richter MF, Sakanari JA, Ozaki LS, et al. Cloning and functional expression of a *Boophilus microplus* cathepsin L-like enzyme. *Insect Biochem Mol Biol* 2000;30:1017–26.
- [9] Sojka D, Hajdusek O, Dvorák J, Sajid M, Franta Z, Schneider EL, et al. IrAE: an asparaginyl endopeptidase (legumain) in the gut of the hard tick *Ixodes ricinus*. *Int J Parasitol* 2007;37:713–24.
- [10] Boldbaatar D, Sikalizyo Sikasunge C, Battsetseg B, Xuan X, Fujisaki K. Molecular cloning and functional characterization of an aspartic protease from the hard tick *Haemaphysalis longicornis*. *Insect Biochem Mol Biol* 2006;36:25–36.
- [11] Motobu M, Tsuji N, Miyoshi T, Huang X, Islam MK, Alim MA, et al. Molecular characterization of a blood-induced serine carboxypeptidase from the ixodid tick *Haemaphysalis longicornis*. *FEBS J* 2007;274:3299–312.
- [12] Alim MA, Tsuji N, Miyoshi T, Islam MK, Hatta T, Fujisaki K. Legumains from the hard tick *Haemaphysalis longicornis* play modulatory roles in blood feeding and gut cellular remodelling and impact on embryogenesis. *Int J Parasitol* 2009;39:97–107.
- [13] Fujisaki K, Kawazu S, Kamio T. The taxonomy of the bovine *Theileria* spp. *Parasitol Today* 1994;10:31–3.
- [14] Hoogstraal H, Roberts FH, Kohls GM, Tipton VJ. Review of *Haemaphysalis* (kaiseriana) *longicornis* Neumann (resurrected) of Australia, New Zealand, New Caledonia, Fiji, Japan, Korea, and Northeastern China and USSR, and its parthenogenetic and bisexual populations (Ixodoidea, Ixodidae). *J Parasitol* 1968;54:1197–213.
- [15] Bowman AS, Sauer JR. Tick salivary glands: function, physiology and future. *Parasitology* 2004;129: 67–81.
- [16] Zaim M, Guillet P. Alternative insecticides: an urgent need. *Trends Parasitol* 2002;18: 161–3.
- [17] Sajid M, McKerrow JH. Cysteine proteases of parasitic organisms. *Mol Biochem Parasitol* 2002;120:1–21.
- [18] von Figura K, Hasilik A. Lysosomal enzymes and their receptors. *J Cell Biol* 1985;101:2253–62.
- [19] Barrett AJ, Kirschke H, Cathepsin B, Cathepsin H, and cathepsin L. *Methods Enzymol* 1981;80: 535–61.
- [20] Dickinson DP. Cysteine peptidases of mammals: their biological roles and potential effects in the oral cavity and other tissues in health and disease. *Crit Rev Oral Biol Med* 2002;13:238–75.
- [21] Tort J, Brindley PJ, Knox D, Wolfe KH, Dalton JP. Proteinases and associated genes of parasitic helminths. *Adv Parasitol* 1999;43:161–266.
- [22] Brady CP, Dowd AJ, Brindley PJ, Ryan T, Day SR, Dalton JP. Recombinant expression and localization of *Schistosoma mansoni* cathepsin L1 support its role in the degradation of host hemoglobin. *Infect Immun* 1999;67:368–74.
- [23] You M, Xuan X, Tsuji N, Kamio T, Taylor D, Suzuki N, et al. Identification and molecular characterization of a chitinase from the hard tick *Haemaphysalis longicornis*. *J Biol Chem* 2003;278:8556–63.
- [24] Bendtsen JD, Nielsen H, von Heijne G, Brunak S. Improved prediction of signal peptide: signal P 3.0. *J Mol Biol* 2004;34:783–95.
- [25] Tsuji N, Kamio T, Isobe T, Fujisaki K. Molecular characterization of a peroxiredoxin from the hard tick *Haemaphysalis longicornis*. *Insect Mol Biol* 2001;10:121–9.
- [26] Turk V, Turk B, Turk D. Lysosomal cysteine proteases: facts and opportunities. *EMBO J* 2001;20: 4629–33.
- [27] Ménard R, Carmona E, Takebe S, Dufour E, Plouffe C, Mason P, et al. Autocatalytic processing of recombinant human procathepsin L. Contribution of both intermolecular and unimolecular events in the processing of procathepsin L in vitro. *J Biol Chem* 1998;273:4478–84.
- [28] Vernet T, Khouri HE, Laflamme P, Tessier DC, Musil R, Gour-Salim BJ, et al. Processing of the papain precursor. Purification of the zymogen and characterization of its mechanism of processing. *J Biol Chem* 1991;266:21451–7.
- [29] Khan AR, James MN. Molecular mechanisms for the conversion of zymogens to active proteolytic enzymes. *Protein Sci* 1998;7: 815–36.
- [30] Taylor MA, Pratt KA, Revell DF, Baker KC, Sumner IG, Goodenough PW. Active papain renatured and processed from insoluble recombinant propapain expressed in *Escherichia coli*. *Protein Eng* 1992;5:455–9.
- [31] Rowan AD, Mason P, Mach L, Mort JS. Rat procathepsin B. Proteolytic processing to the mature form in vitro. *J Biol Chem* 1992;267:15993–9.
- [32] Mason RW, Gal S, Gottesman MM. The identification of the major excreted protein (MEP) from a transformed mouse fibroblast cell line as a catalytically active precursor form of cathepsin L. *Biochem J* 1987;248:449–54.
- [33] McQueney MS, Amegadzie BY, D'Alessio K, Hanning CR, McLaughlin MM, McNulty D, et al. Autocatalytic activation of human cathepsin K. *J Biol Chem* 1997;272: 13955–60.
- [34] Reich CI, Zorzopoulos J. *Boophilus microplus*: characterization of larval proteases. *Exp Parasitol* 1978;44:1–6.
- [35] Mendiola J, Alonso M, Marquetti MC, Finlay C. *Boophilus microplus*: multiple proteolytic activities in the midgut. *Exp Parasitol* 1996;82:27–33.
- [36] Bogin E, Hadani A. Digestive enzymes in hard ticks. Proteolytic enzyme activity in the gut of *Hyalomma excavatum* female ticks. *Z parasitenkd* 1973;41: 139–46.
- [37] McKerrow JH, Sun E, Rosenthal PJ, Bouvier J. The proteases and pathogenicity of parasitic protozoa. *Annu Rev Microbiol* 1993;47:821–53.
- [38] Rosenthal PJ. Hydrolysis of erythrocyte proteins by proteases of malaria parasites. *Curr Opin Hematol* 2002;9: 140–5.
- [39] Tsuji N, Miyoshi T, Battsetseg B, Matsuo T, Xuan X, Fujisaki K. A cysteine protease is critical for *Babesia* spp. transmission in *Haemaphysalis* ticks. *PLoS Pathog* 2008;4: e1000062.
- [40] Hoogstraal H. Argasid and nuttalliellid ticks as parasites and vectors. *Adv Parasitol* 1985;24:135–238.
- [41] de la Fuente J, Kocan KM, Blouin EF. Tick vaccines and the transmission of tick-borne pathogens. *Vet Res Commun* 2007;31:85–90.

## A salivary cystatin, HISC-1, from the ixodid tick *Haemaphysalis longicornis* play roles in the blood-feeding processes

Kayoko Yamaji · Naotoshi Tsuji · Takeharu Miyoshi · M. Khyrul Islam · Takeshi Hatta · M. Abdul Alim · M. Anisuzzaman · Shiro Kushibiki · Kozo Fujisaki

Received: 16 July 2009 / Accepted: 3 September 2009 / Published online: 25 September 2009  
© Springer-Verlag 2009

**Abstract** Ticks feed exclusively on blood to obtain their nutrients, but the gene products that mediate blood-sucking processes in ticks are still unknown. We report here the molecular characterization and possible biological function of a cysteine protease inhibitor (HISC-1) identified in the salivary gland of the ixodid tick *Haemaphysalis longicornis*. The HISC-1 cDNA contains 423 bp that code for 140 amino acids with a predictable molecular weight of 12 kDa. The recombinant HISC-1 expressed in *Escherichia coli* was shown to inhibit the activity of papain and cathepsin L, while cathepsin B activity was unaffected. Immunolocalization studies detected the endogenous enzyme in the salivary gland type II acini of an adult tick. Furthermore, quantitative RT-PCR analysis showed that the expression of *HISC-1* transcripts was associated with blood-feeding processes and was highly up-regulated in the early

phase of feeding. Our results strongly suggest that HISC-1 may play pivotal roles in the blood-feeding processes.

### Introduction

Ticks are able to passively cling to an unsuspecting host, crawl on the skin, insert its mouthpart into the skin, and then create a blood pool from which they siphons their meal over a period of 5 to 7 days. The reason for the complexity and redundancy of tick immunomodulatory factors may be related to the fact that ticks feed for many days and thus need multiple mechanisms to inhibit/circumvent a host's inflammatory/immune response to the tick's presence. For that reason, the adaptation to blood feeding involves evolution of salivary glands that help the tick to overcome

K. Yamaji · N. Tsuji (✉) · T. Miyoshi · M. K. Islam · T. Hatta · M. A. Alim · M. Anisuzzaman  
Laboratory of Parasitic Diseases, National Institute of Animal Health, National Agriculture and Food Research Organization, 3-1-5 Kannondai,  
Tsukuba, Ibaraki 305-0856, Japan  
e-mail: tsujin@affrc.go.jp

K. Yamaji · S. Kushibiki  
Graduate School of Life and Environmental Sciences,  
University of Tsukuba,  
Tennodai,  
Tsukuba, Ibaraki 305-8572, Japan

N. Tsuji · M. Anisuzzaman  
Graduate School of Agricultural and Life Sciences,  
The University of Tokyo,  
Yayoi, Bunkyo-ku,  
Tokyo 113-8657, Japan

S. Kushibiki  
National Institute of Livestock and Grassland Science,  
National Agriculture and Food Research Organization,  
Ikenodai,  
Tsukuba, Ibaraki 305-0901, Japan

K. Fujisaki  
National Research Center of Protozoan Diseases,  
Obihiro University of Agriculture and Veterinary Medicine,  
Inada-cho,  
Obihiro, Hokkaido 080-8555, Japan

K. Fujisaki  
Department of Frontier Veterinary Medicine,  
Kagoshima University,  
Korimoto, Kagoshima 890-0065, Japan

its host's defenses and the development of inflammatory reactions at the feeding site. Saliva of ixodid ticks are thought to contain anticoagulant, antiplatelet, and vasodilatory molecules, all of which inhibit host hemostasis and keep blood flowing at the bite site (Ribeiro 1995; Ribeiro and Francischetti 2003; Sauer et al. 1995).

Cysteine protease inhibitors, cystatins, constitute a large group of evolutionary-related proteins acting as protease inhibitors of papain-like cysteine proteases belonging to enzyme family C1, such as cathepsins B, H, L, and S and legumain-related proteases of the family C13 (Rawlings et al. 2004a). The type 1 cystatins, stefins, are polypeptides of about 100 amino acid residues which possess neither disulfide bonds nor carbohydrate side chains and are located mainly intracellularly. The type 2 cystatins C, D, E/M, F, S, SN, and SA, are characterized by two conserved disulfide bridges, a larger size (~120 residues) and the presence of a signal peptide for extracellular targeting (Rawlings et al. 2004b) and secreted and found in most biological fluids (Vray et al. 2002). The type 3 cystatins, the kininogens, are large (60–120 kDa) multifunctional plasma proteins, containing three type 2 cystatin-like domains having a total of eight disulfide bridges. These inhibitors might protect the cells from inappropriate endogenous or external proteolysis and/or could be involved in the control mechanism responsible for intracellular or extracellular protein breakdown (Turk and Bode 1991; Vray et al. 2002). Recent studies showed that salivary cystatins are characterized from the blacklegged tick *Ixodes scapularis* (Kotsyfakis et al. 2006, 2007) and the lone star tick *Amblyomma americanum* (Karim et al. 2005). Moreover, midgut cystatins of several tick species, including the hard tick *Haemaphysalis longicornis* and the soft tick *Ornithodoros moubata*, have been characterized to date (Grunclová et al. 2006). Previously, cystatins had been characterized from *H. longicornis*, named Hlcyst-1, -2, and -3 in our group (Zhou et al. 2006, 2009). It has implicated that Hlcyst-2 play a role in defense due to their capability to inhibit proteinases from pathogens, and Hlcyst-1 have been suggested as regulators of endogenous proteolytic activities during blood-feeding stage.

We describe here the characterization of a cDNA encoding a salivary cystatin, HISC-1, from the ixodid tick *H. longicornis*, which has a wide geographical distribution in Russia, Eastern Asia, Australia, and New Zealand and the potential to transmit pathogens, including viruses, rickettsia, and protozoan parasites, causing important human and animal diseases (Fujisaki et al. 1994; Hoogstraal et al. 1968). The deduced precursor protein contains amino acids conserved among family 2 members of cystatin group and three cystatin motif. Endogenous HISC-1 was highly expressed in type II acini cells of the salivary glands, and its expression was found to be induced by early phase of the

blood-feeding process. A recombinant HISC-1 was shown to inhibit a wide range of cysteine protease activities, suggesting that HISC-1 may play pivotal roles in the blood-feeding processes by the ixodid ticks.

## Materials and methods

### Ticks and animals

*H. longicornis* (Okayama strain) were maintained at the Laboratory of Parasitic Diseases, National Institute of Animal Health, Tsukuba, Ibaraki, Japan on rabbits as described previously (You et al. 2003). All animals used this study were acclimatized to the experimental conditions for 2 weeks prior to the experiment. Animal experiments at the National Institute of Animal Health (NIAH) were conducted in accordance with protocols approved by the Animal Care and Use Committee, NIAH (approval no. 08-021).

### Cloning and sequencing of *HISC-1*

*HISC-1* was identified from expressed sequence tags constructed from salivary glands cDNA libraries of *H. longicornis* as described previously (Harnnoi et al. 2007). The plasmids containing *HISC-1* gene-encoding inserts were extracted using the Qiagen DNA purification kit (QIAGEN Sciences, Germantown, MA, USA). The nucleotide sequences of the cDNAs were determined by the BigDye Terminator method on an ABI PRISM 3100 automated sequencer (Applied Biosystems, Foster City, CA, USA). The GENETYX-WIN DNA analysis software system (Software Inc.) was used to deduce the amino acid sequence of *HISC-1*. Alignments of protein sequences within other homologues were performed at the DNA Data Bank of Japan (<http://blast.ddbj.nig.ac.jp/top-j.html>). Signal peptide analysis was performed using the SignalP version 3.0 (<http://www.cbs.dtu.dk/services/SignalP>) program (Bendtsen et al. 2004).

### Production of polyclonal sera

The peptide *CGENKGHG* (56 to 62 of *HISC-1*) was coupled to keyhole bovine serum albumin (BSA). Synthetic peptides were used to raise polyclonal antibodies in BALB/c mice by injection of 20 µg of the antigen emulsified with incomplete Freund's adjuvant (Difco Laboratories, Detroit, USA). The antigen administration was repeated at 2 and 4 weeks, and the animals were bled after 6 weeks when antisera were tested by ELISA and Western blotting. Peptides (10 µg) of BSA were diluted in phosphate-buffered saline (PBS) and adsorbed on ELISA 96-well microtiter plates (Nunc) overnight at 4°C. The wells were blocked with PBS, 0.1 %

Tween 20 (*v/v*), and 5% non-fat milk for 90 min at 37°C and incubated for 2 h at 37°C with control PBS, diluted 1:50 in PBS containing 0.1% of Tween 20 (*v/v*). The wells were subsequently washed three times with PBS, 0.1% Tween 20 (*v/v*) and incubated for 1 h at room temperature with alkaline phosphatase-conjugated AffiniPure goat anti-mouse IgG (Jackson Immuno Research, USA; diluted 1:1,000). After washing as described above, the reaction was developed with *o*-phenylenediamine (Bio-Rad) according to manufacturer's instructions and the optical density determined at 492 nm. Antibodies in the serum of these immunized mouse reacted with recombinant HISC-1, but not Hlcyst-1 and Hlcyst-2 in immunoblotting experiments (data not shown).

#### Immunofluorescence staining

For endogenous localization of HISC-1, salivary glands were collected from adult ticks after 48 h of blood feeding. Salivary glands were fixed in 4% paraformaldehyde in 0.1 M phosphate buffer (pH 7.2) for 6 h at 4°C and embedded in paraffin and used to make thin flat sections. The sections on glass slides were blocked with 10% goat serum (MP Biomedicals, Irvine, CA, USA) for 30 min at room temperature, washed twice in PBS, and then incubated with mouse anti-HISC-1 serum diluted 1:500 for 24 h at 4°C. The slides were washed three times with PBS then incubated with green fluorescent-labeled mouse IgG secondary antibody [Alexa Fluor<sup>®</sup>488 goat anti-mouse IgG] (H+L; Invitrogen) for 1 h at room temperature. The slides were observed under a fluorescence microscope (Leica, Wetzlar, Germany).

#### Quantitative RT-PCR

Total RNA was extracted from the midgut and salivary gland of adult ticks with RNeasy mini kit (QIAGEN) following the manufacturer's instructions. cDNA synthesis from total RNA was performed with a Takara RNA PCR kit (AMV) Ver3.0 (Takara Bio Inc., Otsu, Japan). The primer combination was as follows: 5' GGTGGTTGCTGCATA AAGT 3' (forward primer), 5' TACGGTCGTGCAGGTA TTCA 3' (reverse primer) for *HISC-1*. Transcript's abundance was measured with a LightCycler 1.5 (Roche Instrument Center AG, Roikreuz, Switzerland) according to the manufacturer's instructions. Quantitative reverse transcription (RT)-PCR was conducted in LightCycler capillaries (Roche) with a 20- $\mu$ l reaction volume containing 4.6  $\mu$ l of LightCycler FastStart DNA Master SYBR Green (Roche), 3 mM of MgCl<sub>2</sub>, 0.5  $\mu$ M each of forward and reverse primers, and cDNA corresponding to 0.2 ng of total RNA. Expression was normalized against  $\beta$ -actin as an internal control. The mRNA abundance unit was calculated

as the number of mRNA molecules per  $\beta$ -actin mRNA. The data were analyzed by LightCycler Software Version 3.5. The  $\beta$ -actin gene was amplified according to the same procedures and used as a control. Each analysis was done at least in triplicate.

#### Expression and purification of recombinant HISC-1 from *Escherichia coli*

A cDNA encoding the HISC-1 was ligated into the expression vector SYN1255-pColdTF (Takara) and was used to transform *E. coli* BL21. Luria–Bertani medium containing ampicillin (50  $\mu$ g/ml) was inoculated with transformed cells and was incubated at 37°C with shaking until the optical density at 600 nm reached 0.4–0.6. Expression of recombinant bacterium-expressed HISC-1 was induced by addition of 1 mM isopropyl  $\beta$ -D-thiogalactopyranoside (IPTG) at 15°C, and the cells were harvested 24 h later by centrifugation. The cells pellet was resuspended in PBS containing 0.1 mg/ml lysozyme at 5 ml/g of cell pellet and sonicated for 2 min to disrupt bacterial cells. The extract was centrifuged at 8500 $\times$ g for 30 min, and the supernatant was incubated with 10 ml of ProBond<sup>™</sup> Resin (Invitrogen, Carlsbad, CA, USA) for 20 min at 4°C. The fusion proteins with a His tag were purified using a proBond following the manufacturer's instructions and then cleaved with thrombin (Novagen, Madison, USA), and purification was checked by sodium dodecyl sulfate polyacrylamide gel electrophoresis (SDS-PAGE). After the cleavage reaction, thrombin was removed with streptavidin agarose (Novagen). The cDNA fragments spanning the *Hlcyst-1* and *Hlcyst-2* ORF (Zhou et al. 2006, 2009), devoid of their signal peptide sequence, were amplified by PCR with AmpliTaq Gold DNA polymerase (Applied Biosystems) and appropriate oligonucleotide primers, *Hlcyst-1* forward: 5' CCGGAATTCGGATGCC TAT GGTGGAGGACT 3', reverse: 5' CCGCTCGAGC GGGTCACTGGAAATGATTGAGTG 3' and *Hlcyst-2* forward: 5'CCGGAATTCGGGGCTGGCGAGACCAG GATCC 3', reverse: 5' CCGCTCGAGCGGGTTACACG CAGTCGAATGAAG 3', which contained a *EcoRI* and a *XhoI* enzyme restriction site. PCR conditions were 30 s at 95°C, 30 s at 55°C, and 2 min at 72°C for 35 cycles. A final 5-min extension was performed at 72°C. The PCR product was inserted in frame into the fusion expression vector pGEX-6p-1 (GE Healthcare Bio-Sciences AB, Piscataway, NJ, USA). *E. coli* BL21 (Invitrogen) containing the recombinant plasmids were grown in SOB medium at 37°C to an OD<sub>550</sub> of approximately 0.5 and induced with 1 mM IPTG for 6 h. The fusion proteins with a GST tag were purified using a glutathione sepharose 4B (GE Healthcare) following the manufacturer's instructions and then cleaved with PreScission Protease (GE Healthcare),

and purification was checked by SDS-PAGE. Total protein concentration was determined by BCA protein assay kit (Thermo Electron Corporation, Waltham, MA, USA).

#### Protease inhibition assays

To measure the inhibitory activity of recombinant HISC-1, the concentration of HISC-1 at which 50% inhibition of the activity of the proteolytic enzymes is achieved ( $IC_{50}$ ) were presented. Recombinant HISC-1 (10–100 pmol) were pre-incubated with each enzyme in an assay buffer for 30 min. Then, 0.25 mM of the protease-specific substrates was added to each well and residual enzyme activity monitored. Assay buffer and enzymes used were as follows: 100 mM sodium acetate, pH 5.5, 100 mM NaCl, 1 mM EDTA, 1 mg/ml cysteine, and 0.01% TritonX-100 for human cathepsin L (Calbiochem, Darmstadt, Germany) and cathepsin B (Sigma, St. Louis, USA); 0.05 M Tris-HCl, pH 7.4, 0.1 M NaCl, and 100  $\mu$ M EDTA for papain (Sigma) and trypsin (Sigma). Substrates purchased from Peptide Institute (Osaka, Japan) were as follows: Z-Phe-Arg-MCA for cathepsin L; Z-Arg-Arg-MCA for cathepsin B; Bz-L-Arg-pNA-HCl for papain and trypsin. Data were fit to the appropriate equation using GraphPad Prism version 4.0 (GraphPad Software, CA, USA). Chromogenic assays were monitored by SPECTRAFLUOR (TECAN, Maennedorf, Switzerland) at 405 nm of absorption. Fluorescence intensity was monitored with the wavelength pair of 360–465 nm for emission and excitation, respectively.

## Results

### HISC-1 encodes a cystatin-like homologue in *H. longicornis*

Recently, with the examination of the *H. longicornis* salivary gland cDNA library (Harnnoi et al. 2007), we have identified a novel cystatin-like homologue, named HISC-1. The cDNA encoding the gene product was amplified from *H. longicornis* RNA by RT-PCR, subcloned, and sequenced. The 423-bp cDNA encoded a HISC-1 having 140 amino acids and contained three putative cystatin motifs at positions 5 (P-I motif), 48–52 (P-II, QxVxG motif), and 105–106 (P-III, PW motif; Fig. 1, box). This deduced protein has a possible cleavable signal peptide of 28 amino acid residues, and the mature protein has a predicted molecular mass of 12,375.44 Da and an isoelectric point ( $pI$ ) value of 9.82. The HISC-1 sequence has been deposited in the GenBank™ database under accession number AB510962.

Figure 1 depicts a comparison of the primary sequence for the novel protein with other tick cystatins and chicken

cystatin; the latter was included in this alignment because its structure and function have been studied extensively (Colella et al. 1989). HISC-1 displayed similarity to family 2 cystatins, such as cystatin C, D, S, SA, and SN, which function as cysteine protease inhibitors. The best hits found with HISC-1 were observed with Hlcyst-2 (38% identity) from *H. longicornis* and for the Omcystat 2 from the argasid tick *O. moubata* (32% identity; Grunclová et al. 2006).

### Localization of endogenous HISC-1

The peptide *CGENKGGH* (italicized letters; 56 to 62 of HISC-1) was used as antigen to produce polyclonal antibody in mice. The resulting serum was able to recognize recombinant HISC-1 on Western blot and ELISA. The anti-HISC-1 antibodies were used to characterize the localization of endogenous HISC-1 by immunofluorescence microscopy (Fig. 2). Tick sections (control) incubated with the same concentration of pre-immune mouse sera and second antibody did not show any positive reaction by immunofluorescence microscopy (Fig. 2, lower panel). These results demonstrated that the novel cystatin homolog present in *H. longicornis* was preferentially localized in the salivary gland type II acini cells (Fig. 2, upper panel). Type II acini are thought to secrete pharmacologically active compounds into the host. This acini contained 14–15 granular cells, all of which surrounded a central lumen which opened via a cuticular valve into a lobular duct (Kemp et al. 1982; Fawcett et al. 1986). Immunolocalizations for HISC-1 was confirmed in the salivary gland type 2 acini area, indicating its secretion into the host tissues during blood feeding early stage. In addition to the result of immunolocalizations, putative signal peptide sequence was identified in the HISC-1 cDNA, suggesting that HISC-1 is secreted.

### *HISC-1* is differentially expressed in the blood-feeding stages

In order to perform a comparative study of the relative abundance of the *HISC-1* transcripts during different phases of blood feeding, a real-time RT-PCR analysis was performed using total RNA extracted from the unfed and partially fed (24, 48, 72, and 96 h) adult *H. longicornis*. The normalized values (Fig. 3) show that the HISC-1 transcripts are abundant in the salivary glands, corresponding to approximately five to tenfold higher amount than in midguts. Furthermore, a dramatic up-regulation of HISC-1 transcripts was recorded in the early phase of blood feeding (24 h), which then gradually declined as feeding progresses and reached a minimal level when ticks achieve a full blood meal.